Renewable Energy 242 (2025) 122388

Contents lists available at ScienceDirect

Renewable Energy

journal homepage: www.elsevier.com/locate/renene

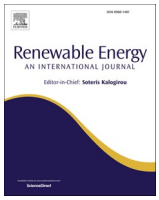

Techno-economic evaluation of pyrolysis and electrolysis integration for methanol and char production

Rafael Nogueira Nakashima [a,*], Hossein Nami [c], Arash Nemati [a], Giacomo Butera [d], Silvio de Oliveira Junior [e], Peter Vang Hendriksen [a,b], Henrik Lund Frandsen [a,b]

[a] Department of Energy Conversion and Storage, Technical University of Denmark (DTU), Building 310, Fysikvej, Lyngby, DK-2800, Denmark
[b] University of Denmark, Denmark
[c] SDU Life Cycle Engineering, Department of Green Technology, University of Southern Denmark, Campusvej 55, 5230, Odense M, Denmark
[d] Stiesdal SkyClean A/S, Vejlevej 270, 7323, Give, Denmark
[e] Department of Mechanical Engineering, Polytechnic School, University of São Paulo, Av. Prof. Luciano Gualberto 380, 05508-010, São Paulo, Brazil

ARTICLE INFO

Keywords:
Pyrolysis
Electrolysis
Methanol
Char
Power-to-Methanol

ABSTRACT

The pyrolysis technology enables the conversion of biomass into different products, such as char, oil, and synthesis gas. These products can play an important role in the decarbonization of agriculture, industry, and transportation, but are challenged by the availability of biomass and low fuel productivity. Electrolysis technologies, such as alkaline or solid oxide electrolysis, can help to overcome these drawbacks by supplying hydrogen derived from renewable sources. This paper focuses on providing the modeling, methods, and analysis necessary to pinpoint the benefits and challenges of this process concept. Integrating electrolysis with pyrolysis greatly improves the carbon conversion efficiency from 65 % to 97.1–97.8 % by increasing the methanol production by 2.7 times. For instance, the integration of co-electrolysis (i.e., CO_2 and H_2O electrolysis) and pyrolysis can increase carbon conversion from 65 % up to 98 %, while attaining a maximum energy efficiency of 67 % (for methanol production). Moreover, projected methanol production costs are estimated to vary between 706 and 922 USD/t for current technology prices. Char plays an important role in abating biomass costs and enabling net negative emissions in methanol production (−0.62 to −1.02 t_{CO2}/t_{CH3OH}). Further improvements can be achieved by optimizing electrolysis operating conditions and by reducing energy consumption in distillation and CO_2 capture.

1. Introduction

Biomass is a renewable source of energy and carbon that can be used to reduce fossil fuel dependence for different products in transportation and industry alongside with other renewable resources. However, the availability of biomass falls short when compared to the global demand for complete decarbonization [1–3]. In general, biomass conversion into chemicals has lower efficiency than solutions based on natural gas [4], which limits the productivity of biorefineries and imposes challenges to their economic competitiveness. In addition, for many proposed schemes a significant portion of the carbon originating from biomass is converted into emitted carbon dioxide instead of being captured or converted into products [5]. This limits the environmental benefits of biomass applications, which could attain negative emission status by combining with carbon storage solutions [6]. Furthermore, if sustainable carbon becomes a scarce resource, then the value of it will increase, and emission of sustainable carbon will also decrease the economic competitiveness of these solutions. Thus, different process designs and improvements have been proposed to increase productivity and environmental benefits of biomass conversion into valuable substances, like methanol, petrol, or jet fuel.

In parallel, hydrogen production using electrolysis has been sought as a pathway to utilize the increasing wind and solar energy capacity for decarbonizing the industry and transportation sectors. The current main technologies for electrolysis are alkaline water electrolysis (AWE), proton exchange membrane electrolysis (PEMEC) and solid oxide cell

* Corresponding author. Department of Energy Conversion and Storage, Technical University of Denmark (DTU), Building 310, Fysikvej, Lyngby, DK-2800, Denmark.
E-mail addresses: rafnn@dtu.dk (R. Nogueira Nakashima), hon@igt.sdu.dk (H. Nami), arnem@dtu.dk (A. Nemati), gbu@stiesdal.com (G. Butera), soj@usp.br (S. de Oliveira Junior), pvhe@dtu.dk (P. Vang Hendriksen), hlfr@dtu.dk (H.L. Frandsen).

https://doi.org/10.1016/j.renene.2025.122388
Received 20 May 2024; Received in revised form 27 December 2024; Accepted 9 January 2025
Available online 10 January 2025

electrolysis (SOEC). Alkaline water electrolysis is the most mature technology available, achieving intermediary efficiency (63–70 % LHV) and long stack lifetimes (>60 kh), while SOEC offers the highest efficiency metrics (74–81 % LHV) with shorter replacement time (<30 kh) and higher investment cost [7]. Despite their differences, a recent study of Nami et al. [8] have indicated that both technologies will achieve similar levelized cost of hydrogen in the following decades (1.4–2 EUR/kg). On the other hand, PEMEC technology's ability to achieve high pressure hydrogen production under a flexible operation range offers a good synergy with e-fuel production and integration with renewable energy sources [9].

Nonetheless, the production of hydrogen for e-fuels requires a high electricity consumption which translates into high e-fuel costs, even in low electricity cost scenarios. Thus, an alternative to reduce energy costs is to use cheap biomass resources to partly provide the energy required for e-fuels. For instance, instead of using carbon dioxide to produce e-methanol, using synthesis gas derived from biomass would reduce the needs for carbon capture and partially cover the hydrogen required for synthesis. Methanol produced in this hybrid pathway is usually label as bio-e-methanol and it could serve as alternative fuel for ships, or chemical input to produce green chemicals, including olefins that could be turned into sustainable aviation fuels [10]. Recently, research efforts have been devoted to exploring the use of electrolysis to boost renewable fuel production from biomass, as presented in the following.

Tock et al. [11] compared the technical and economic prospects of converting biomass into liquid fuels, estimating a 52.5 % energy efficiency and 128 EUR/MWh (709 EUR/t) cost for methanol production. Their research also highlighted how the CO_2 removal unit may limit the energy integration of the system. Lebaek et al. [12] discussed the limitations of "conventional" biorefineries in converting biomass carbon into products and proposed the integration with electrolysis which can increase methanol production by more than a factor of two. In addition, their report pointed to an increase in energy efficiency (70.8 %) and an estimated methanol cost of 141 USD/barrel eq. (approx. 527 USD/t). Ali et al. [13] pinpointed additional benefits on integrating solid oxide electrolysis (SOEC) with syngas reforming for methanol production. The switch from steam reforming to autothermal reforming, enabled by the oxygen produced by the electrolysis unit, can significantly reduce energy demand and increase the rate of the methanol synthesis reaction.

Zhang et al. [14] evaluated the trade-offs of methanol production using biomass and SOEC technology in comparison with a state-of-the-art biorefinery. Their research indicated that the minimal methanol production cost (336 USD/t) was attained by a state-of-the-art biorefinery exporting electricity and methanol. Higher efficiencies and lower biomass consumption can be achieved by integrating electrolysis, but methanol costs sharply increased with higher carbon conversion. Butera et al. [15,16] proposed a flexible system using gasification and SOECs that can adapt to changes in electricity prices to store or produce electricity when economically viable. The flexible system requires a significantly higher investment cost compared to conventional solutions, but it can achieve similar methanol costs with higher capacity factor and methanol yield.

Few studies have explored the possible integration of biomass and electrolysis with focus on pyrolysis. One of the main advantages of this technology is the production of char alongside synthesis gas. Char can be used as either a solution for energy storage or for carbon storage. It is however more likely that char will be used for carbon storage, as the energy otherwise is better stored in a gaseous or liquid fuel. Currently biochar is envisaged by the Danish government to be as the biggest contributor in the green transition of the agricultural sector in Denmark [17]. Abandoning char gasification (as in the gasification technology) also increases the pyrolysis heating demand and reduces the production of the synthesis gas. The storage of carbon in the form of biochar thus comes with an energy cost, as compared to storing CO_2 (although CO_2 capture and storage may be quite energy intensive as well). Depending on the pyrolysis feedstock and processing conditions, biochar is converted slowly over hundreds of years [18]. Thus, if biochar is continuously produced, a large fraction of it can be considered as a storage of carbon. Furthermore, biochar has been proven useful as a fertilizer, potentially increasing the soil fertility and productivity [19].

Pyrolysis gas may on the other hand be used as an energy product in the supply of heat, power and/or in the production of biofuels such as methanol. To maintain high productivity of energy products from the same feedstock, pyrolysis can be integrated with electrolysis. This can increase biofuel production by providing hydrogen for stoichiometric correction of the syngas and, in some cases, supply high temperature heat. However, a detailed evaluation of this process design compared with the conventional bio-methanol production plant has not been investigated so far for pyrolysis technology. In addition, the techno-economic trade-offs between traditional and emerging electrolysis technologies have also seldom been addressed.

Thus, this research aims to provide an in-depth comparison of the techno-economic perspectives of pyrolysis combined with electrolysis for methanol production and hereby range from pure bio production to different e-bio-methanol technologies. The study compares the integration of pyrolysis with different scalable electrolysis technologies, including the alkaline electrolysis technology, the steam solid oxide electrolysis and the carbon-dioxide/steam co-electrolysis technology. The main novelties of this work can be summarized as: (i) detailed techno-economic modelling of 4 different routes of methanol production, including 3 different electrolysis technologies (ii) detailed 1D+1D modeling of co-electrolysis of CO_2 using solid oxide cell technology (iii) a mixed integer linear optimization method for energy integration alongside technology selection and sizing (iv) a benchmark comparison between numerous results in literature normalized for the same economic assumptions.

This study is organized in five main sections: Introduction, Methods, Energy integration optimization, Results and Conclusions. The next section details the description of each process and the main modeling assumptions. The optimization methods and key performance indicators are explained in section 3, followed by results and discussions in section 4, and conclusions in section 5.

2. Methods

This research evaluates the integration of three different types of electrolysis technologies, i.e. , alkaline water electrolysis and high temperature solid oxide electrolysis operating with steam or a CO_2/CO/H_2O/H_2 mixture (co-electrolysis), for methanol production using carbon derived from straw pyrolysis. In addition, a base case consisting of methanol production from straw pyrolysis without hydrogenation using electrolysis is also considered as a benchmark case. Thus, three routes using electrolysis to recover carbon into methanol are compared with a base case without electrolysis. A general process flowsheet of the methanol plant including the pyrolysis, reforming and methanol synthesis is shown in Fig. 1. A detailed explanation of each process unit is given in the following subsections.

2.1. Pyrolysis

In the pyrolysis process, illustrated in Fig. 1, straw pellets are thermochemically converted into char and gas by exposing biomass to a high temperature environment operating close to atmospheric pressure (1.05 bar), in absence of added oxygen. Depending on biomass type and operating conditions, the pyrolysis reactions may be slightly endothermic or exothermic. The reactor temperature (500 °C) is maintained by recycling and reheating the gas stream (from ca. 300 °C to 500 °C). Char represents one of the main products of the process. It enables stable carbon sequestration and contains all the nutrients initially present in the biomass to be recirculated to the crop of origin. Conversely, harmful substances (e.g. hormone-like substances and antibiotics) are broken down at pyrolysis temperature. To ensure the production of high-quality

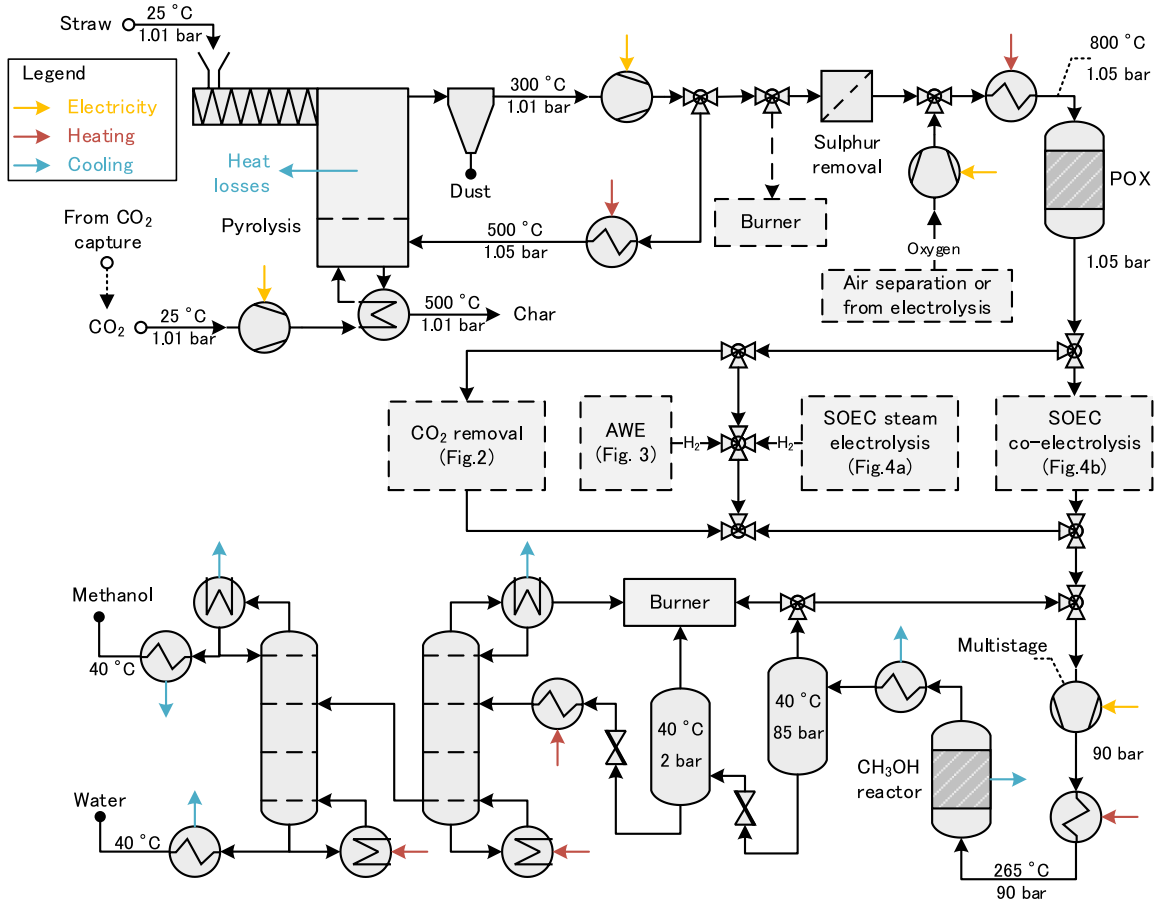

Fig. 1. General process flowsheet of the methanol plant excluding utilities and syngas treatment (some streams were omitted so simplify the diagram).

tar-free char, an inert (e.g., N_2, H_2O or CO_2) is used to avoid pyrolysis gas and tar vapor sticking to the char. In the proposed process, CO_2 is chosen as the inert gas to avoid recirculating N_2 in the methanol synthesis and simpler implementation compared to steam, which would require a more complex heating system. The design of the pyrolysis systems is based on the TwoStage Viking gasifier developed in the Technical University of Denmark [20] and previously studied by Butera et al. [16].

The pyrolysis reactor is modelled based on the conservation of species and assuming that the energy flow rate (lower heating value basis) of the products is equal to the dry reactants [15]. Furthermore, the concentration of certain species in the products are fitted to match, as close as possible, the composition measured experimentally for the dry pyrolysis gases [15], as presented in Table A 1. The mathematical model for the pyrolysis reactor was developed in EES V11 [21].

2.2. Partial oxidation reforming (POX)

The partial oxidation reformer converts hydrocarbons (e.g., methane, ethane, ethylene, propane, among others) into CO, CO_2 and H_2 to avoid undesirable reactions (i.e., cracking and carbon formation) and large temperature drops in the downstream processes. The reactor design is divided into two parts: a combustion zone (Pt/Al_2O_3) and a reforming/shift zone (Ni/Al_2O_3) [22]. The process proposed for gas reforming is illustrated in Fig. 1.

The methanol synthesis reaction requires 2 mol of H_2 per mole of CO and 3 mol of H_2 per mole of CO_2. For syngas mixtures, this stoichiometric relation is usually defined based on the S ratio, as described in Eq. (1), which should be equal to 2 for methanol production. Thus, the reforming unit aims to increase S by converting hydrocarbons into hydrogen and carbon monoxide. Thus, the oxygen to carbon ratio in the partial oxidation reforming is optimized to maximize the S ratio of the reformed gas.

$$S = \frac{\dot{n}_{H_2} - \dot{n}_{CO_2}}{\dot{n}_{CO_2} + \dot{n}_{CO}} \tag{1}$$

S stoichiometric ratio for syngas mixtures.
$\dot{n}_j$ molar flow rate of specie j, kmol/s.

To avoid contamination of the reforming catalysts, sulfur is removed from the pyrolysis gas using metal oxide beds [15]. The reactor inlet temperature is fixed to 800 °C and oxygen mass flow rate is controlled to maximize the stoichiometric ratio of syngas for fuel production. For scenarios using electrolysis, pure oxygen is supplied from the electrolysis unit while in the base scenario it is supplied from an air separation unit. The assumptions and parameters for the reforming unit are summarized in Table A 2.

The partial oxidation reformer is modelled in Aspen Plus V11 [23] as an adiabatic plug-flow reactor with partial combustion reactions for methane and higher hydrocarbons. The rate of reaction for methane partial oxidation as proposed by Marechal et al. [22]. All higher hydrocarbons (C_xH_y) are assumed to be partial oxidized. In addition, the water gas shift and steam methane reforming reactions are assumed to be in chemical equilibrium at the outlet of the reformer. The reactor size is designed iteratively to reach the same outlet composition given by chemical equilibrium under adiabatic conditions. The thermodynamic properties of gases are calculated using the Soave-Redlich-Kwong

equation of state, as in previous literature [24].

2.3. Carbon dioxide separation

In the base scenario of this study, excess carbon dioxide (CO_2) is separated by an amine absorption unit to reach the targeted S ratio, as illustrated in Fig. 2. However, since the CO_2 concentration in the reformed syngas may be low, an additional conditioning step is required. A water gas shift reactor using 10 % Fe/Al_2O_3 catalyst is introduced to convert CO and H_2O into H_2 and CO_2 [22]. High pressure steam (15 bar) is added to the reformed syngas to increase the steam to carbon ratio to safe operating levels.

The amine absorption unit, illustrated in Fig. 2, uses an aqueous solution (33 % wt.) of methyldiethanolamine (MDEA) to remove CO_2 from the gas in an absorber column. The amine solution is then regenerated in a two-step process, i.e., depressurization and stripper, with the latter using an external heat supply (i.e., steam). Makeup water and MDEA are supplied to the regenerated solution to maintain the amine concentration. Table A 3 summarizes the main parameters and assumptions for this unit.

The amine absorption unit model was developed in Aspen Plus V11 [23]. The water gas shift reactor is modelled as an adiabatic plug-flow reactor as proposed by Ref. [22]. On the other hand, chemical equilibrium is used to determinate the carbon formation limit (S/C = 1.13 in this case). The thermodynamic properties of gases mixtures were calculated using Soave-Redlich-Kwong equation of state.

The amine absorption model is based on Refs. [25,26], but the absorber and stripper sizes were adapted for the specific needs of this application, such as pressure and final CO_2 concentration. Thermodynamic properties of the ionic components and the liquids are estimated by using the electrolyte non-random two liquid model (ELECNRTL), with parameters calibrated from binary vapor-liquid equilibrium data [26].

2.4. Alkaline water electrolysis (AWE)

The electrolysis unit aims to supply the hydrogen required to convert all carbon available in the reformate gas, which avoids the separation of excess carbon as is required in the base scenario. Alkaline water electrolysis is the most mature electrochemical technology for hydrogen production and, therefore, exemplifies the base scenario for methanol production assisted by electrolysis. The electrolysis system, illustrated in Fig. 3, employs a liquid electrolyte (KOH 30 % wt.) and a zero-gap design for membrane-electrode assembly, which operates at 80 °C and atmospheric pressure. The liquid electrolyte is recycled together with the makeup water and the temperature is controlled by an auxiliary cooling system.

The thermodynamic model estimates the cell voltage based on a pseudo-empirical model with 4 calibration parameters, as proposed by Jin et al. [27] based on previous studies of Ulleberg [28]. In addition, Faraday efficiency was modelled as proposed by Ulleberg [28] with refitted parameters. A comparison between the developed model results and experimental data reported by Ulleberg [28] is shown in Fig. 4.

The voltage equation was implemented as a 0D model in Aspen Plus V11 [23], assuming negligible temperature and concentration differences across the cells, a valid simplification for operating conditions with small temperature variations as shown in previous studies [27]. The model estimates the electrolyte properties by using the ELECNTRL mixture model with default binary coefficients. Moreover, the heat of electrochemical reaction is estimated from the energy balance, Eq. (2), including the effect of the Faraday efficiency on the mass balance. The electrolyte mass flow rate is determined iteratively by fixing a maximum temperature difference of 1 °C across the stack.

$$Q_r = n_{cells}\left(V - V_{tn}\eta_{faraday}\right)jA_{cell} \tag{2}$$

Q_r heat of reaction, W.
n_{cells} total number of cells, -.
V_{tn} thermoneutral voltage, V.
A_{cell} active cell area, m^2.

2.5. Solid oxide electrolysis (SOE)

Among the different electrolysis technologies, this study considers the use of solid oxide electrolysis cells (SOECs) due to their high efficiency for both steam electrolysis and co-electrolysis. In addition, since SOECs operate at high temperatures (>600 °C), this technology has more possibilities for integration with other thermochemical conversion processes (e.g., pyrolysis, reforming, methanol synthesis). Fig. 5 illustrates, the steam electrolysis and co-electrolysis designs.

In steam electrolysis, only water and a fraction of recycled products are used to produce hydrogen, while for the co-electrolysis case, one uses reformed syngas and steam. Therefore, the definition of feedstock utilization (FU) for steam electrolysis had to be extended to include CO_2, CO, and CH_4, as shown in Eq. (3). Steam consumption in the co-electrolysis was determined iteratively by fixing the feedstock utilization efficiency and thermoneutral voltage.

$$FU = \frac{\left(\dot{n}_{H_2,o} - \dot{n}_{H_2,i}\right) + \left(\dot{n}_{CO,o} - \dot{n}_{CO,i}\right)}{\dot{n}_{CO_2,i} + \dot{n}_{H_2O,i} + 3\dot{n}_{CH_4,i}} \tag{3}$$

$\dot{n}_{x,i}$ inlet molar flow rate of specie “x”, mol/s.
$\dot{n}_{x,o}$ outlet molar flow rate of specie “x”, mol/s.

Although the solid oxide cells can also reform methane, the direct reforming of methane is reduced by partial oxidation to avoid steep temperature gradients in the cells, as shown in fuel cells [29]. Both designs produce oxygen as a side-product, which is partially consumed

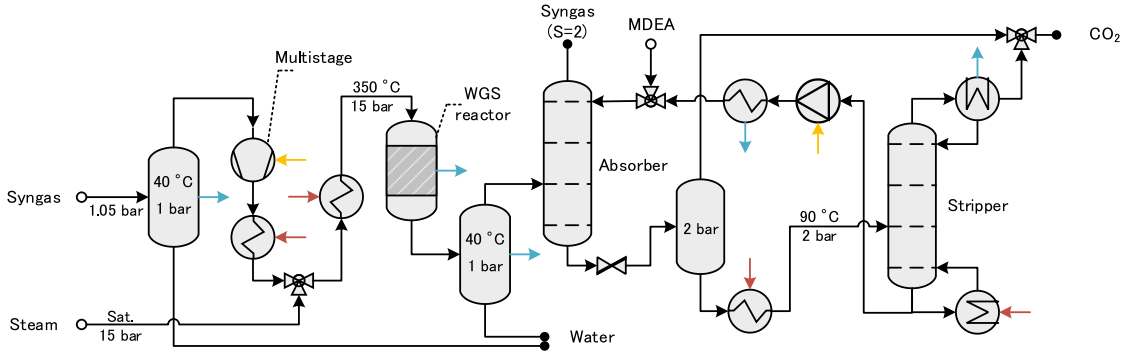

Fig. 2. Process flow diagram of the amine absorption unit.

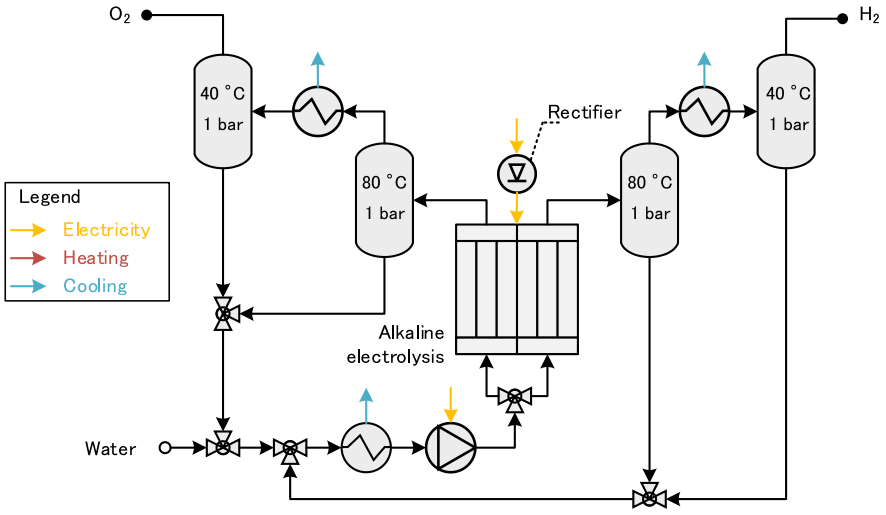

Fig. 3. Process flow diagram of the alkaline water electrolysis unit.

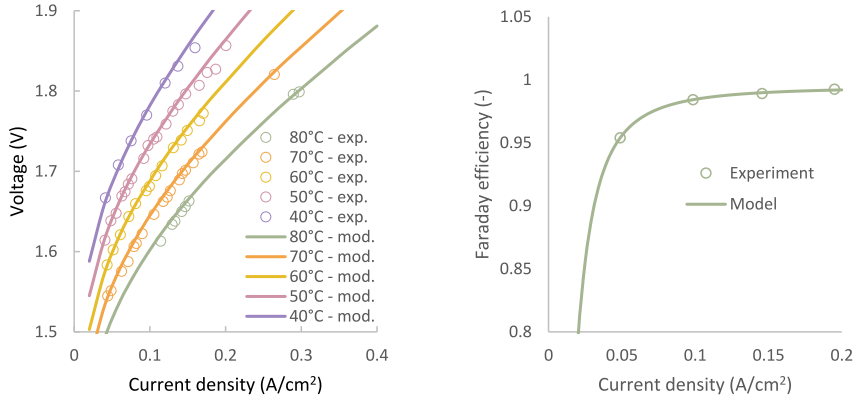

(a) Polarization curve (b) Faraday efficiency

Fig. 4. Alkaline water electrolysis model validation with data from Ref. [28].

in the reforming unit. It should be noted that, although SOECs have been demonstrated to operate with pure oxygen, the operation with oxygen at system level is still in development due to the difficulties in handling O_2 at high temperatures. A summary of the main assumptions adopted in the modelling of the electrolysis units is presented in Table A 4.

A quasi-2D model for solid oxide fuel cells developed in a previous work [30,31] was updated to model the electrolysis process. The dusty gas diffusion model was implemented to describe the transport of species in the porous electrodes [32]. In addition, the electrochemistry model was also modified according to the equations and parameters proposed by Nami et al. [8], which are summarized in Table A 5. The comparison of the model results with experimental data is shown in Fig. 6.

The co-electrolysis process is simplified as a combination of water electrolysis and water gas shift reactions, as there are no in-depth investigations of the different competing reaction mechanisms. The water gas shift reaction rate proposed by Haberman and Young [33] was used to estimate the changes in fuel composition along the cells length. As seen in Fig. 11, there are some minor deviations between the resulting model and experimental data for co-electrolysis (Fig. 11b), when compared to the accuracy for steam electrolysis (Fig. 11a), but the simplifications proposed in this study can reproduce the polarization curve trends with reasonable accuracy. The steam electrolysis and co-electrolysis units were modelled in the Julia programming language [34]. The details of the thermodynamic and transport properties can be found in Refs. [30,31].

2.6. *Methanol synthesis and distillation*

The methanol synthesis unit, shown in Fig. 1, is based on the isothermal reactor design with a high recycle ratio to maximize methanol yield and recover energy as high temperature steam. Methanol is separated from water in a two-step distillation process to attain fuel grade purity. The unconverted portion of syngas is recirculated, while a fraction is bled to avoid concentration of undesired species. That fraction is burned, and the heat delivered to the heat recovery system. The main modelling parameters for the methanol synthesis unit are presented in Table A 6.

The methanol production is modelled as an isothermal reactor (265 °C, 90 bar) from the stoichiometric mixture of carbon dioxide, carbon monoxide and hydrogen. The chemical reactor is designed to achieve the same product's composition at 20 °C below the chemical equilibrium condition, as obtained in previous works [35]. The reaction rate is estimated based on the model proposed by Bussche and Froment

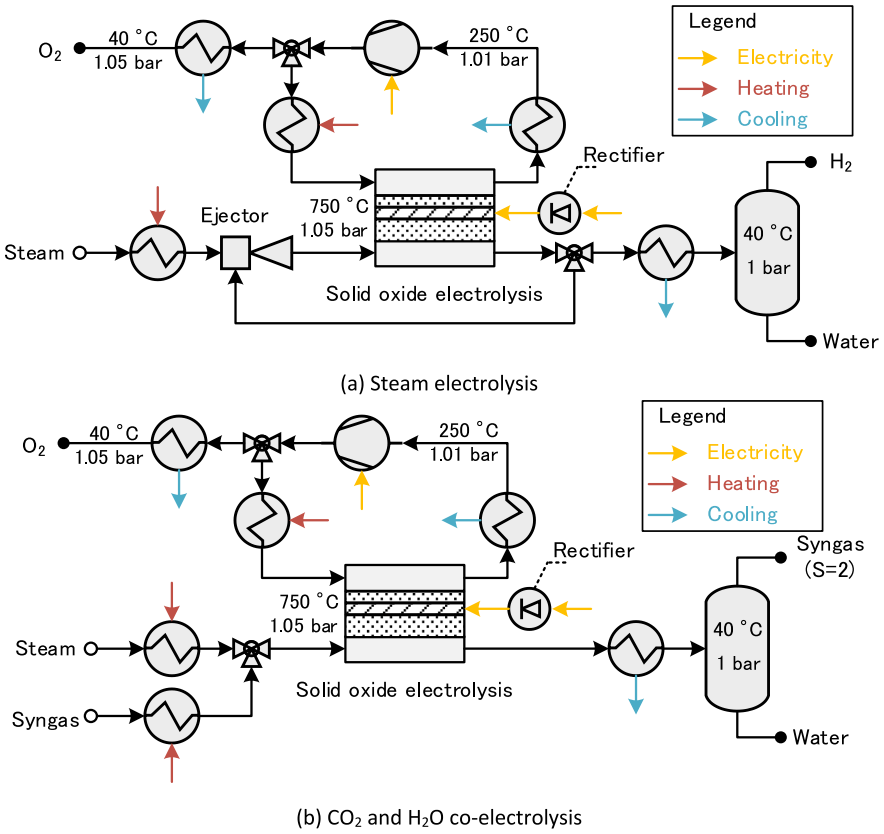

Fig. 5. Process flow diagram of solid oxide electrolysis.

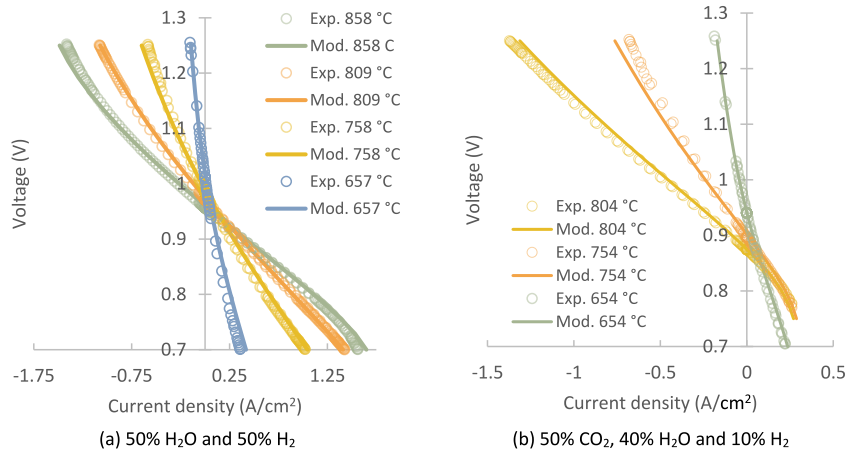

Fig. 6. Model results compared with experimental data (operation with pure O_2) from DTU-Energy for cells with LSCF-CGO electrodes [8].

[36] for a copper/zinc oxide catalyst [37]. The thermodynamic properties for gas and liquid mixtures are estimated using Soave-Redlich-Kwong equation of state with calibrated parameters for methanol-water mixtures [37].

2.7. Utilities

The combustion of fuels (i.e., straw and pyrolysis gas) or purge gas can provide heat at high temperatures for different processes. A generic burner is modelled as a combination of fan, heat exchanger and reactor assuming complete oxidation of the fuel. On the other hand, the energy consumption connected with water vaporization is estimated by a simple model consisting of a pump and heater. Other utility units, such as cooling water, air separation, and electric heating, are modelled as black boxes using data reported in the literature. Table A 7 summarizes the main modelling assumptions for all utility units.

3. Energy integration optimization

For each scenario in this study, the process and utility units are sized considering the possible energy integrations between them. The linear optimization problem described in Eqs. (4)–(7) determines the scale factors (f) for each unit that maximize the hourly profits (Eq. (4)). The main constraints in the problem are: (i) the balance of resources (Eq. (5)), (ii) the heat cascade (Eqs. (6) and (7)), and the piece-wise linearization of capital investment (Eqs. (8)–(11)) [38–40]. A simplified

diagram exemplifying the problem of a single unit and two resources is illustrated in Fig. 7.

$$\max_{r_i^{in}, r_i^{out}, f^\tau, y^\tau, R_k} \underbrace{\sum_i^I \left(r_i^{out} c_i^{out} - r_i^{in} c_i^{in}\right)}_{resources} - \underbrace{\sum_\tau^{\tau_n} \sum_s^S \left(f_s^\tau a_{GR,s}^\tau + y_s^\tau b_{GR,s}^\tau\right) \frac{(\beta_{CRF} + \beta_{COM})}{t_{op}}}_{investment\ \&\ fixed\ expenses} \quad (4)$$

Subjected to:

$$r_i^{in} + \sum_\tau^{\tau_n} f^\tau \left(r_i^{\tau,in} - r_i^{\tau,out}\right) = r_i^{out} \quad \forall i \in resources \quad (5)$$

$$R_{k-1} + \sum_\tau^{\tau_n} f^\tau \left(\sum_n^N Q_{n,k}^\tau\right) = R_k \quad \forall k \in [1, \ldots, K] \quad (6)$$

$$\begin{matrix} R_k = 0, k = 0, K \\ R_k \geq 0, otherwise \end{matrix} \quad (7)$$

$$f^\tau = \sum_s^S f_s^\tau \quad \forall \tau \in units \quad (8)$$

$$\sum_s^S y_s^\tau \leq 1 \quad \forall \tau \in units \quad (9)$$

$$f_{s,min}^\tau y^\tau \leq f_s^\tau \leq f_{max}^\tau y^\tau \quad \forall \tau \in units \quad (10)$$

$$y_s^\tau \in \{0, 1\} \quad (11)$$

r_i input (in) or output (out) resource rate for the overall system or unit τ, kg/h or kW.
c_i specific cost of resource input (in) or output (out), USD/kg or USD/kWh.
t_{op} yearly operating hours, h/year.
f^τ size factor of unit τ, -.
y_s^τ binary variable associated with the choice of unit τ and segment s, {1,0}.
$a_{GR,s}$ slope linear constant for the cost of a new facility (i.e., "grassroots" costs) associated with unit τ and segment s, USD.
$b_{GR,s}$ intercept linear constant for the cost of a new facility (i.e., "grassroots" costs) associated with unit τ and segment s, USD.
β_{CRF} capital recovery factor, 1/year.
β_{COM} cost of manufacturing factor (taxes, insurance, and maintenance), 1/year.
R_k residual heat transfer of temperature interval 'k', kW.
$Q_{n,k}^\tau$ heat transfer rate of stream 'n' of unit 'τ' at temperature interval 'k', kW.
$f_{s,max}^\tau, f_{s,min}^\tau$ maximal (max) or minimal (min) size factor of unit 'τ', -.

3.1. Cost modelling

In this optimization problem, the hourly operating profits are estimated assuming an amortization of the fixed investment capital, which is calculated using a capital recovery factor with an effective discount rate [41]. In the electrolysis scenarios, the number of operating hours in these cases were reduced from 7200 h/year to 4380 h/year to account for the capacity factor of approximately 50 % of combined renewable electricity sources. The general economic assumptions for this study are summarized in Table 1.

Cost correlations proposed by Seider et al. [46], Turton et al. [41] and others [8,16] are assumed to determine the equipment cost for a specific size at design conditions. It is important to highlight that replacement costs for catalysts and stacks are also summed up with the purchase costs by converting the future payments into present value, as described by Ref. [8]. A detailed description of the cost for each equipment is provided in the supplementary material.

Since the heat exchanger pairs are not defined in the pinch analysis, the heat exchanger cost can only be roughly estimated in the linear optimization problem. In this study, a heat exchanger area is associated with each stream assuming that all heat transfer occurs at the pinch temperature. This represents the worst-case scenario of the method

Table 1
General economic assumptions.

Parameter	Value
Yearly operating hours (t_{op})	Base case: 7200 h/year [42] Others: 4380 h/year [8]
Project lifetime (n)	20 years [41]
Discount rate (i)	8 % [43]
Inflation rate (i_{inf})	2 % [44]
Cost of manufacturing factor (β_{COM})	Property taxes: 2 % C_{GR} Insurance: 1 % C_{GR} Maintenance 6 % C_{GR} [45]
Number of operators per shift (N_{OL})	Pyrolysis + Reforming: 4 Carbon capture/Electrolysis: 2 Methanol plant: 2 [46]
Direct labor costs (C_{OL})	$4.5\left[\frac{operators\ hired}{operators\ per\ shift}\right] \cdot 70,000 \left[\frac{USD}{y\ .\ operator\ hired}\right] \cdot N_{OL}$ [43]
Overhead charge	125 % C_{OL} [45]
Year reference for costs	2022
Cost index (CEPCI)	816 [47,48]

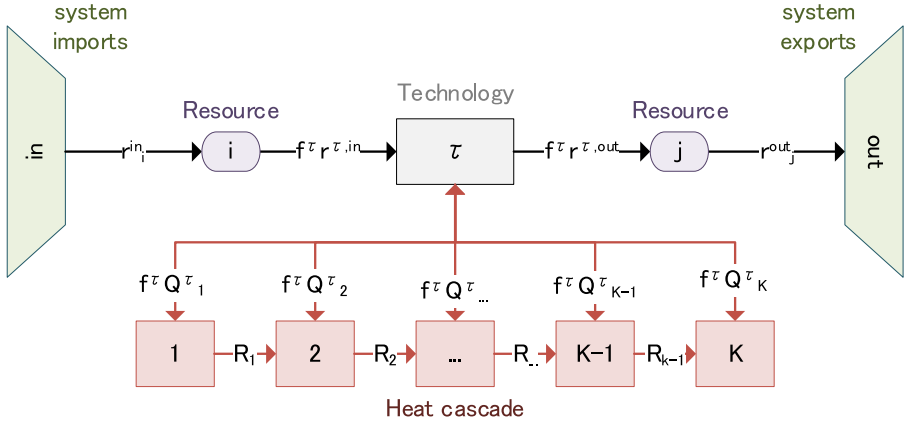

Fig. 7. Diagram of the optimization problem for a single unit 'τ' and two resources 'i' and 'j'.

usually employed to estimate the heat exchanger area of temperature intervals [41]. The individual film heat transfer coefficients are estimated based on typical heat transfer coefficients reported by Turton et al. [41] and the assumed values are presented on Table 2.

The term "grassroots" is used throughout this study to refer to the costs of a completely new facility in an undeveloped land following the nomenclature proposed by Turton et al. [41]. In practice, this means that the fixed capital investment will assume an additional costs (50 % of the sum of the bare module costs at reference conditions [41]) to cover for auxiliary facilities costs. The costs for building a new facility (i.e., "grassroots" costs) vary non-linearly with size, as the cost equations are rarely linear functions.

However, it is possible to approximate the effects of economy of scale by a linear regression in restricted intervals. In the optimization problem, this approach is extended to create a piece-wise linearization of the "grassroots" costs including multiple segments, as proposed by other authors [40]. A detailed presentation of the linearization of "grassroots" costs is provided in supplementary material.

In this study, the pyrolysis unit size was fixed to operate with 400 MW of straw in lower heating value. The boundary conditions of the optimization problem are specified as fixed resources to be imported or exported by the overall system, as presented in Table 3. It is important to note that water is assumed to be completely reused in the processes whenever available with no treatment cost. In addition, char revenues are calculated based on a carbon credit of 120 USD/t of CO_2 emissions avoided, based on February 2023 values for European carbon permits [49]. The carbon abatement is estimated as equivalent to 85 % of carbon contained in char [18]. Similarly, the cost for CO_2 for the pyrolysis reactor is estimated from the carbon credits, although it could also be supplied internally from the carbon capture or distillation units.

The methanol costs are calculated iteratively from the optimization results as the minimal selling price to achieve a net zero hourly operating revenue.

3.2. Performance indicators

The technical performance of each scenario is mainly evaluated using exergy analysis. The exergy efficiency (η_{ex}), defined in Eq. (12), is based on the rational definition: the sum of exergy outputs divided by the sum of exergy inputs. Since water and oxygen represent relatively small contributions in the exergy balance, their values can be omitted from the exergy efficiency definition for simplicity.

$$\eta_{ex.I} = \frac{B_{methanol} + B_{char}}{B_{straw} + W_{total}} \tag{12}$$

B_i exergy flow rate related to resource "i", kW.
W_{total} total power consumption, kW.

Similarly, an energy efficiency (η_{en}) definition is provided in Eq. (13) for comparison with other energy analysis studies. In Eq. (13), the energy flow rate of resources is determined using the lower heating value basis (LHV), since most studies report energy efficiency using this assumption. In addition, the effect of humidity in the LHV of straw is estimated by subtracting the energy required for water vaporization, as described in Eq. (14).

Table 2
Individual film heat transfer coefficient assumption.

Stream type	Film heat transfer coefficient [kW/m^2.K]
Gas	60
Liquid	560
Condenser	1700
Reboiler	2280

Table 3
Resources cost base assumptions[a].

Resource	Import cost	Export cost	Ref.
Straw	111 USD/t (7.3 USD/GJ)	–	[16]
Char	–	267 USD/t	[18,49]
Water	0.11 USD/t	0 USD/t	[41]
Oxygen	–	0 USD/t	–
Electricity	60 USD/MWh (16.7 USD/GJ)	–	[50]
CO_2	120 USD/t	–	[49]
Methanol	–	Calculated	–

[a] Exchange rates of 6.29 DKK/USD [51] and 1.14 EUR/USD [52].

$$\eta_{en.I} = \frac{E_{methanol} + E_{char}}{E_{straw} + W_{total}} \tag{13}$$

E_i energy flow rate (LHV) related to resource "i", kW.

$$LHV_{straw} = (1 - \phi)LHV_{dry} - \phi\Delta h_{vap} \tag{14}$$

LHV_{straw} lower heating value in humid basis, kJ/kg.
LHV_{dry} lower heating value in dry basis, kJ/kg.
ϕ humidity (mass basis), kg_{water}/kg.
Δh_{vap} specific enthalpy change for water vaporization, kJ/kg.

A second definition for exergy and energy efficiency excluding the char from the products is also calculated for comparison with other studies, as described respectively in Eqs. (15) and (16). In this case, the exergy/energy content of the char is subtracted from the exergy/energy of the straw.

$$\eta_{ex.II} = \frac{B_{methanol}}{B_{straw} - B_{char} + W_{total}} \tag{15}$$

$$\eta_{en.II} = \frac{E_{methanol}}{E_{straw} - E_{char} + W_{total}} \tag{16}$$

Carbon conversion efficiency (η_{carbon}) is defined as the ratio of carbon in products (methanol and char) per carbon in feedstock (straw). This ratio can be calculated as exemplified in Eq. (17) and aims to provide an environmental performance indicator. Furthermore, as carbon from biomass could well become a scarce resource [1], future plants should be optimized to utilize the available carbon as good as possible. As the value of carbon in such a society is highly uncertain, this has not been included in the economic optimization.

$$\eta_{carbon} = \frac{\dot{c}_{MeOH} + \dot{c}_{char}}{\dot{c}_{straw}} \tag{17}$$

$\dot{c}_i$ mass flow rate of carbon in resource "i", kg/s.

3.3. Benchmark analysis

It is important to highlight that the economic assumptions taken by other authors are different than those taken in this present study. This usually limits the validity of comparing the estimated fuel costs and significantly hinders a generalization of the economic results. Therefore, in this study a benchmark cost definition is proposed, as defined in Eq. (18), that aims to include the CAPEX, main consumptions, and products to compare several studies under the same economic assumptions. The proposed equation uses commonly reported technical-economic parameters, such as investment per methanol production rate (USD/kW) and specific consumptions and by-products per methanol produced.

$$c_{benchmark} = CAPEX\left(\frac{LHV^{*}CRF}{t_{op}}\right) + \gamma_b c_b + \gamma_e c_e - \gamma_c c_c \tag{18}$$

$c_{benchmark}$ benchmark cost of methanol, USD/t
CAPEX total investment cost, USD/kW
LHV lower heating value of methanol, kWh/t
CRF Capital recovery factor, 1/y
γ_b, γ_e, and γ_c specific consumption/production of biomass [GJ/t], electricity [MWh/t] and char [t/t]
c_b, c_e, c_c costs of biomass [USD/GJ], electricity [USD/MWh] and char [USD/t]

4. Results

In this section, the results are presented in two different perspectives: technical and economic. Furthermore, the key performance indicators are compared with values reported by previous studies in a discussion subsection.

4.1. Technical perspectives

The balance of products and consumptions, as well as efficiencies for each scenario are summarized in Table 4. It is noticeable that the bio-e-methanol scenarios, which include an electrolysis unit, have a substantial higher production of methanol (≥270 %) compared to base scenario, representing a conventional bio-methanol plant, given a fixed available amount of straw feedstock. The addition of hydrogen to syngas increases the productivity of methanol, since carbon dioxide does not need to be separated from pyrolysis gas to attain the stoichiometric ratio for methanol synthesis. This difference can also be observed by comparing the carbon conversion efficiencies of electrolysis scenarios (≥97 %) with the base case (65 %), as shown in Table 4. However, the higher carbon conversion is also connected to a higher electricity consumption, 4.8–6.5 MWh/t_{CH3OH}, approximately 5.7–7.8 times higher than the base scenario (0.84 MWh/t_{CH3OH}). Thus, electrolysis can help to address the limited availability of biomass resources for fuel production, if renewable electricity is available to supplement biomass as energy input.

The results presented in Table 4 also indicate that the energy and exergy efficiency indicators vary significantly depending on how char is accounted in the efficiency definition. For instance, the exergy efficiency of the co-electrolysis scenario is estimated to be 77 % including char as an energy product (Definition I), but, if char is discounted from the biomass consumption (Definition II), the exergy efficiency drops to 69 %. Char will likely be used more often as a carbon storage alternative, although it could also be an energy storage solution, therefore the first definition of energy/exergy efficiency may be considered too optimistic. The second definition of energy/exergy efficiency aims to provide a parameter which can be better compared to bio-e-methanol plants that entirely convert biomass into methanol (e.g., gasification-based plants). However, it should be highlighted that, in definition II, all inefficiencies of pyrolysis are attributed to methanol production, instead of being split between both products, methanol and char. Therefore, energy and exergy efficiencies using definition II will likely be lower than values reported for bio-e-methanol plants solely producing methanol.

Among the presented scenarios in Table 4, co-electrolysis (CE-SOC) achieves the highest efficiencies indicators, which are closely followed by the steam electrolysis (SE-SOC). These scenarios can achieve higher efficiencies due to: (i) its lower power consumption for electrolysis (≤4.98 kWh/t_{CH3OH}) compared to alkaline water electrolysis (AWE), and (ii) lower straw consumption (≤1.58 t/t_{CH3OH}) compared to the base scenario. Char represents a significant energy/exergy output of the system (i.e., 24–46 % of energy input and 48 % of biomass energy), as it can be seen by comparing the first definition for only methanol with total (methanol + char). For instance, in the base scenario, methanol accounts for only 29.6 % points of a total of 75.4 % points in energy efficiency.

A detailed breakdown of the power consumption for each scenario is provided in Table 5. The data indicates that gas compression and electrolysis are the main power consumptions for the base and bio-e-methanol scenarios, respectively. In this study, pyrolysis and electrolysis are assumed to operate close to environmental pressure, while methanol synthesis is performed at 90 bar. The large difference in pressure between these systems drives the power consumption of gas compression upwards. On the other hand, the power consumption of the electrolysis stack is connected to the hydrogen demand and operating conditions of the reaction. For instance, steam and co-electrolysis (SOC) present similar power consumptions since they operate at similar conditions for the same hydrogen demand. Alkaline water electrolysis is estimated to have a 47 % higher power consumption due to the lower operating temperature of the technology and assumed current density (0.5 A/cm^2).

The results summarized in Table 5 also indicate a significant contribution of the electric heating to the total electricity consumption. This energy consumption is directly connected with the energy integration of the processes, which can be illustrated from the grand composite curves of Fig. 8. The pinch analysis shows that all scenarios lack high temperature heat (>260 °C) within the processes and, therefore,

Table 4
Products, consumptions, and efficiencies for each scenario.

		Scenario			
		Base	Alkaline water electrolysis	Steam electrolysis (SOC)	Co-electrolysis (SOC)
Products					
Methanol	t/h	22.02	59.50	59.50	60.27
Char	t/t_{CH3OH}	1.12	0.41	0.41	0.41
Oxygen	t/t_{CH3OH}	–	0.61	0.61	0.60
Consumptions					
Straw	t/t_{CH3OH}	4.26	1.58	1.58	1.56
Electricity	MWh/t_{CH3OH}	0.84	6.53	4.98	4.80
Water	t/t_{CH3OH}	–	0.42	0.44	0.43
CO_2	t/t_{CH3OH}	–	0.08	0.08	0.08
Efficiencies					
Energy I	Only methanol	29.6 %	42.1 %	47.7 %	48.8 %
	Total	75.4 %	66.2 %	75.1 %	76.5 %
Exergy I	Only methanol	29.6 %	44.4 %	50.0 %	51.1 %
	Total	72.7 %	68.4 %	76.9 %	78.2 %
Carbon	Only methanol	20.0 %	54.2 %	54.2 %	54.9 %
	Total	65.0 %	97.1 %	97.1 %	97.8 %
Energy II	–	54.6 %	55.5 %	65.7 %	67.5 %
Exergy II	–	52.0 %	58.4 %	68.4 %	70.1 %

Table 5
Electricity consumption distribution.

Consumption [MWh/t_{CH3OH}] (%)	Scenario			
	Base	Alkaline water electrolysis	Steam electrolysis (SOC)	Co-electrolysis (SOC)
Electrolysis stack - DC	–	4.98 (76 %)	3.38 (68 %)	3.37 (70 %)
AC/DC conversion	–	0.26 (4 %)	0.18 (4 %)	0.18 (4 %)
Gas compression	0.62 (75 %)	0.61 (9 %)	0.61 (9 %)	0.59 (12 %)
Electric heating	–	0.57 (9 %)	0.74 (9 %)	0.60 (12 %)
Air separation	0.06 (7 %)	–	–	–
Others	0.16 (19 %)	0.10 (2 %)	0.07 (2 %)	0.07 (1 %)
Total	**0.84 (100 %)**	**6.53 (100 %)**	**4.98 (100 %)**	**4.80 (100 %)**

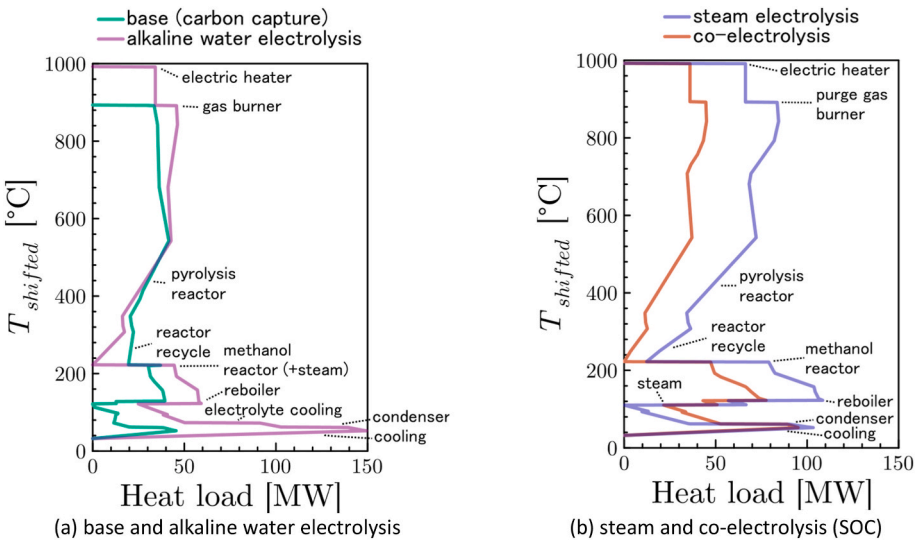

Fig. 8. Comparison of the grand composite curves for different scenarios.

this energy needs to be supplemented either by burning pyrolysis gas (base scenario) or an electric heater (electrolysis scenarios). This feature is particular of this pyrolysis-based system, since most designs for methanol production use gasification, in which the exothermal reactions offer heat energy at high temperatures. Thus, the electric heater covers mostly the high temperature energy demands, such as pyrolysis reactor and methanol recycle loop, since the methanol reactor can provide energy for the low temperature processes such as distillation and steam generation. This explains why AWE and CE-SOC scenarios have similar electric heating consumptions (Table 5) despite co-electrolysis requiring steam as an input. Reducing the pyrolysis reactor temperature could have minor benefits in the heat integration, slightly reducing the electric heating, but it would also be detrimental for the char composition (i.e., less stable carbon retention in the soil).

Other differences between the scenarios which can be observed from Fig. 8 are: (i) a higher heat demand at high temperatures for the steam electrolysis scenario and (ii) a higher heat supply from the methanol reactor for the electrolysis scenarios. The first difference can be explained by the higher steam demand of steam electrolysis compared to co-electrolysis, which is heated up to 750 °C, alongside with the higher mass flow rate entering the methanol reactor, due to the higher concentration of carbon dioxide. The syngas used for methanol synthesis in co-electrolysis and the base scenario have higher concentrations of CO because of the use of the water gas shift reaction and, specifically in base case, the carbon dioxide removal. A comparison between the different scenarios regarding the steam consumption for electrolysis and inlet gas composition for methanol synthesis is presented in Table 6. The second difference can be attributed to the higher production of methanol of electrolysis-based scenarios, which derives from an exothermal reaction, as previously shown in Table 5.

The exergy destruction analysis, shown in Fig. 9, pinpoints major improvement opportunities for the utilities. This can be explained by the fact that the utilities include highly irreversible processes, such as gas combustion and electric heating. There are several possible improvements that could reduce the exergy destruction, which can be categorized as: (i) improving efficiency (ii) reducing the heating demands. For example, the cogeneration of power and heat is a usual solution for improving the efficiency of the heat recovery system. Some solutions proposed in literature include the use of Rankine cycles [14], gas turbines [53], internal combustion engines [54], and heat pumps [15]. On the other hand, reducing the heating demands could be achieved by optimizing some operating conditions for specific components, such as feedstock utilization in SOCs or recycle ratio in methanol synthesis, or

Table 6
Steam consumption for electrolysis and inlet gas of methanol synthesis of each scenario.

	Scenario			
	Base	Alkaline water electrolysis	Steam electrolysis (SOC)	Co-electrolysis (SOC)
Steam consumption for electrolysis [t/h]	–	–	71.8	47.8
Inlet syngas in methanol synthesis				
H_2 (% molar)	76.7	81.4	81.4	85.8
H_2O (% molar)	<1	<1	<1	<1
CO (% molar)	7.4	6.0	6.0	7.5
CO_2 (% molar)	5.9	7.4	7.4	6.2
CH_4 (% molar)	9.6	4.9	4.9	0.1
CH_3OH (% molar)	0.3	0.3	0.3	0.3
Flow rate [kmol/s]	3.58	8.18	8.18	7.07

by changing the technology of certain processes. For example, (i) using physical absorption for CO_2 removal, or (ii) including multiple distillation steps, could eliminate/reduce the heat demand for reboilers in separation. Another possible solution for the AWE and CE-SOC cases is to export steam for other purposes, such as district heating or anaerobic digestion.

Fig. 9 also highlights the large difference between solid oxide cells and alkaline water electrolysis. The exergy destruction of AWE is estimated to be 4 times higher than for steam or co-electrolysis, due to the large fraction of electricity being converted into low temperature heat. Interestingly, the exergy destruction analysis also shows that the co-electrolysis by itself generates as much irreversibilities as steam electrolysis, however the synergies with methanol synthesis and utilities reduce the total exergy destroyed and increase efficiency. For instance, co-electrolysis generates syngas with lower concentrations of methane, reducing losses in the purge gas, and reduce the heat demand for steam generation and superheating, as discussed previously with Table 6. Thus, this indicates that co-electrolysis technology benefits are intertwined with process integration and, therefore, must be analyzed together with fuel synthesis as done here. It should also be noted that a reduction in the heat demand of methanol distillation, for instance by increasing the number of stages or by employing heat pumps, could potentially reduce the gap between steam electrolysis and co-

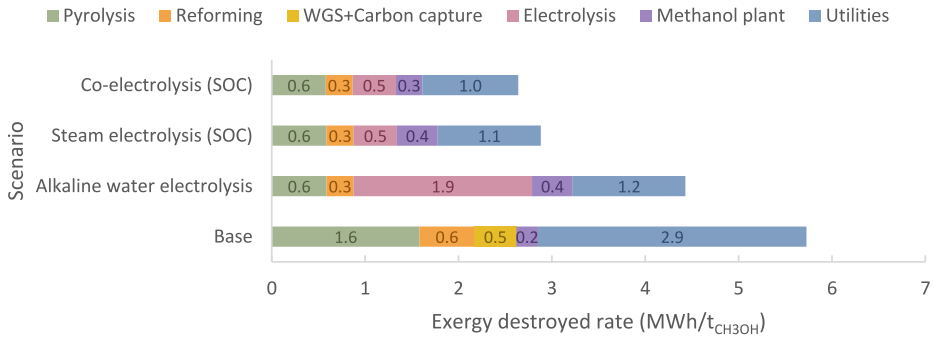

Fig. 9. Exergy destruction assessment for each scenario.

electrolysis by reducing the irreversibilities in the utilities.

Finally, the direct CO_2 production related to the consumption of straw, excluding the indirect emissions from electricity generation, are presented in Table 7. Unlike most methanol plants, all scenarios proposed in this study have a net negative CO_2 in the production step thanks to the char co-production. The CO_2 production for the base scenario are higher than the bio-e-methanol plants, due to the losses in carbon capture and combustion of pyrolysis gas for heating. For instance, if the captured CO_2 in base case could be stored or repurposed, the CO_2 produced per metric ton of straw could be reduced by 193 %. For the scenarios including electrolysis, the CO_2 could be theoretically further reduced if the purge gas from methanol synthesis was recycled back to the reforming step. It is important to highlight that the CO_2 production accounted in Table 7 is derived from biogenic sources and, therefore, the positive values may not account as direct emissions but as null contributions.

4.2. Economic perspective

The methanol cost breakdown for each route is shown in Fig. 10, including the usual range of uncertainty for CAPEX estimations, according to Turton et al. [41]. For current electrolysis prices (Table 1), the production costs of methanol using pyrolysis gas vary between 706 and 922 USD/t, among which the lowest value is attained by the base case scenario (706 USD/t), which represents a conventional bio-methanol plant. For the electrolysis scenarios, methanol costs are estimated to be 21–31 % higher than bio-methanol, reaching as low as 856 USD/t with co-electrolysis technology.

It is noticeable that the biomass cost (straw) is 170 % higher for base scenario (474 USD/t) than the electrolysis-based solutions (174 USD/t), since the hydrogen and heat required to produce methanol are provided solely from straw. On the other hand, the electrolysis routes have 474–680 % higher costs associated with electricity consumption (from 288 to 392 USD/t), because electrolysis and electric heating drive the electricity consumption upwards (Table 5). Furthermore, the carbon credits from the production of char are responsible for decreasing the methanol cost in 109–298 USD/t, as shown in Fig. 10. The revenues derived from the carbon credits of char represent 63 % of biomass costs for the assumed prices in this analysis (Table 2).

Fig. 10 also indicates that the fixed capital investment (FCI) of the process plant is estimated to represent 22–29 % of methanol costs (203–212 USD/t) and impacts indirectly on additional 23–30 % related to taxes, insurance, and maintenance costs (according to assumptions stated in Table 1). It is important to highlight that the estimates for equipment costs are subjected to a usual uncertainty of −25 %/+40 %, which widens the range of fuel costs from 595 to 1077 USD/t. Nevertheless, the contribution of FCI to methanol cost corroborates with the range reported by IRENA [10] from 206 to 293 USD/t for bio-methanol from biomass. An assessment of the fixed capital investment for each scenario is presented in Table 8 for comparison.

Despite the higher capital investment, the bio-e-methanol scenarios have similar specific costs (from 203 to 212 USD/t) compared with the base scenario (205 USD/t), due to the high methanol production rate (Table 4). This is quite remarkable since the electrolysis scenarios are assumed to operate only half of the year on full load condition, against approx. 82 % for the base scenario (Table 1). In addition, Table 8 shows that the most expensive equipment can be categorized into: (i) pyrolysis, (ii) compressors, (iii) heat exchangers, and (iv) electrolysis stack and rectifier. As discussed for the exergy destruction analysis, changing operating and design parameters (e.g., methanol synthesis pressure and

Table 7
Direct CO_2 production excluding electricity generation.

CO_2 production [t/t$_{straw}$]	Scenario			
	Base	Alkaline water electrolysis	Steam electrolysis (SOC)	Co-electrolysis (SOC)
Char	−0.69	−0.69	−0.69	−0.69
CO_2 separation	0.29	0.00	0.00	0.00
Syngas burner	0.24	0.00	0.00	0.00
Methanol synthesis	0.02	0.05	0.05	0.04

Table 8
Estimated fixed capital investment for each scenario.

Cost [USD] (USD/t$_{CH3OH}$)	Scenario			
	Base	Alkaline water electrolysis	Steam electrolysis (SOC)	Co-electrolysis (SOC)
Bare module				
Pyrolysis	81 (44)	81 (27)	81 (27)	81 (26)
Compressors	35 (19)	60 (20)	60 (20)	58 (19)
Heat exchangers	32 (17)	53 (18)	65 (22)	55 (18)
AWE stack	–	57 (19)	–	–
SOC stack	–	–	78 (26)	87 (28)
Rectifier	–	52 (17)	35 (12)	36 (12)
POX reactor	9 (5)	12 (4)	12 (4)	12 (4)
WGS reactor	21 (11)	–	–	–
Air separation unit	20 (11)	–	–	–
Gas burner	10 (5)	4 (1)	4 (1)	3 (1)
Other – Processes	9 (5)	28 (9)	23 (8)	20 (7)
Other – Utilities	9 (5)	18 (6)	23 (8)	17 (5)
Contingency	34 (18)	55 (18)	57 (19)	55 (18)
Fees	7 (4)	11 (4)	11 (4)	11 (4)
Auxiliary facilities	112 (61)	182 (60)	190 (63)	184 (60)
Total fixed capital investment	377 (205)	612 (203)	640 (212)	620 (203)

recycle ratio) could also reduce the size of compressors and heat exchangers and, consequently, their costs. For instance, the minimal temperature approach has a large effect on the heat exchanger area and the numbers assumed in this study could be optimized. It should be highlighted that although AWE and SOC scenarios have similar "grass-roots" costs, the replacement cost for SOC is $\geq$ 4.1 times higher than for alkaline electrolysis, as shown previously in Fig. 10.

It should be noted that the methanol produced and the operating hours for each scenario are different and this impacts the estimated methanol costs, as depicted in Fig. 11. The economy of scale slightly favors the bio-e-methanol scenarios compared with the base scenario, but they are not as impactful as the number of operating hours. For instance, if the electrolysis-based system operated the same number of hours of the base case (for instance, by using energy storage) the methanol production could be reduced by 19–23 % compared to the reference values presented in Fig. 11. This result emphasizes the need to devise operating strategies and/or energy storage solutions that could maximize the capacity factor of electrolysis-based systems to reduce costs in Power-to-X projects. For example, the e-bio-methanol plant can operate flexible according to the availability or cost of electricity [16], or include energy storage systems to increase capacity factor [55], or rely on hydrogen grid and/or super grid [56].

Moreover, the influence of electricity, straw, carbon credits and stack costs also have a significant impact on the methanol costs, as illustrated in Fig. 12. As can be observed, bio-methanol produced in the base scenario prevails as the cheapest route for a wide range of studied costs. However, under low electricity prices, high biomass costs and lower stack costs, the bio-e-methanol scenarios close the gap of cost difference. This indicates that bio-e-methanol production will more likely be fostered by an increase in renewable methanol demand, which will drive fuel prices upwards making higher productivity more economic attractive, rather than a cost saving aspect for biomass-based plants. Larger demand will also promote e-bio-methanol, as biomass is likely to become a limitation, as the pure bio-methanol base system only produces a third of the methanol with the same amount of biomass (see Table 4). It is also interesting to note that, under low electricity prices (<25 $/MWh), alkaline electrolysis becomes the most attractive bio-e-methanol route, since this drastically reduces its operational costs. Thus, reducing stack costs and the frequency of replacements have an important role in making solid oxide cells more competitive as electrolysis technology.

Fig. 13 illustrates the region in which the methanol costs in base scenario is lower than in e-bio-methanol cases for different electricity costs, straw costs, and operating hours. The electricity cost threshold is defined as the value in which the cost of methanol (c_{CH3OH}) equals the value for the base scenario ($c_{CH3OH,base}$). For instance, at the reference straw costs (7.3 USD/GJ) and operating 4380 h/y, the e-bio-methanol routes produce less expensive methanol when electricity costs are below 22 USD/MWh (threshold value). This threshold rises as the straw cost and/or operating hours increase, meaning that bio-e-methanol plants become more economically attractive compared to bio-methanol plants at a wider range of electricity prices.

4.3. Benchmark analysis results

Table 9 summarizes data from 22 scenarios of 8 recent studies for bio-methanol and bio-e-methanol plants, including the present work. Overall, the benchmark fuel cost allows us to visualize certain trends among the scenarios and some outliers, as illustrated in Fig. 14. Under the economic assumptions stated in Tables 1 and 3, bio-methanol plants usually present lower fuel costs and carbon conversion efficiency than e-bio-methanol plants. The systems based on solid oxide electrolysis present a higher efficiency than PEM and alkaline electrolysis, but very similar carbon conversion efficiencies. It is interesting to note that the pyrolysis-based system proposed here presents relatively high carbon conversion efficiencies for bio-methanol plants, due to char production, and competitive costs when compared with among bio-e-methanol plants.

In comparison with values reported in literature, it is possible to observe that the design proposed in this present study consumes more biomass and electricity per metric ton of methanol when comparing similar scenarios. The main explanation for this trend is the high production of char in the pyrolysis-based design, which directs part of biomass and its energy to this alternative carbon capture solution, rather than methanol or heat and power. In addition, some of the previous studies may have opted for different operating conditions and utilities technologies, such as engines [54], gas turbines [53] or Rankine cycle [14]. Most of the values for CAPEX in Table 9 are in the range values reported compiled by IRENA [10], from 1620 to 4280 USD/kW, for bio-methanol plant projects between 100 and 300 kt/y. Despite the high cost of electrolysis, the specific CAPEX of bio-e-methanol plants are usually lower than bio-methanol due to the higher productivity.

4.4. Discussion

Previous studies have also demonstrated how electrolysis can increase the production of methanol from biomass gasification. For instance, Clausen [5] has estimated an increase of 206–216 % by integrating electrolysis with biomass gasification for methanol production. In the previous section, the methanol output is estimated to be 270 % higher for bio-e-methanol plants compared to the base scenario. The difference in percentage increase can be attributed to the partial

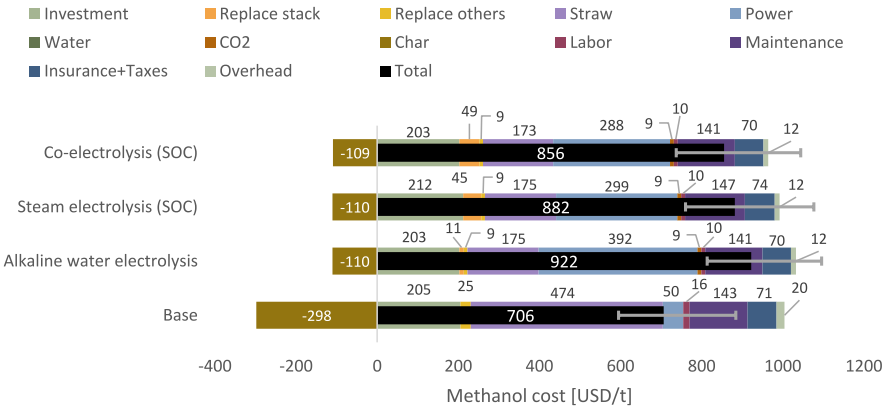

Fig. 10. Fuel cost including usual range for CAPEX estimations (+40 %/−25 %) - $C_{GR,\ AEC} \approx 641$ USD/kW, $C_{GR,\ SOEC\text{-}SE} \approx 1014$ USD/kW and $C_{GR,\ SOEC\text{-}CE} \approx 1087$ USD/kW.

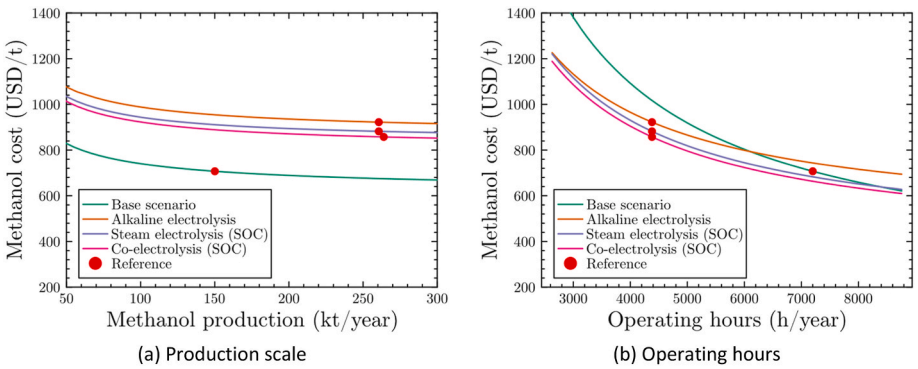

Fig. 11. Influence of production scale and operating hours on methanol cost.

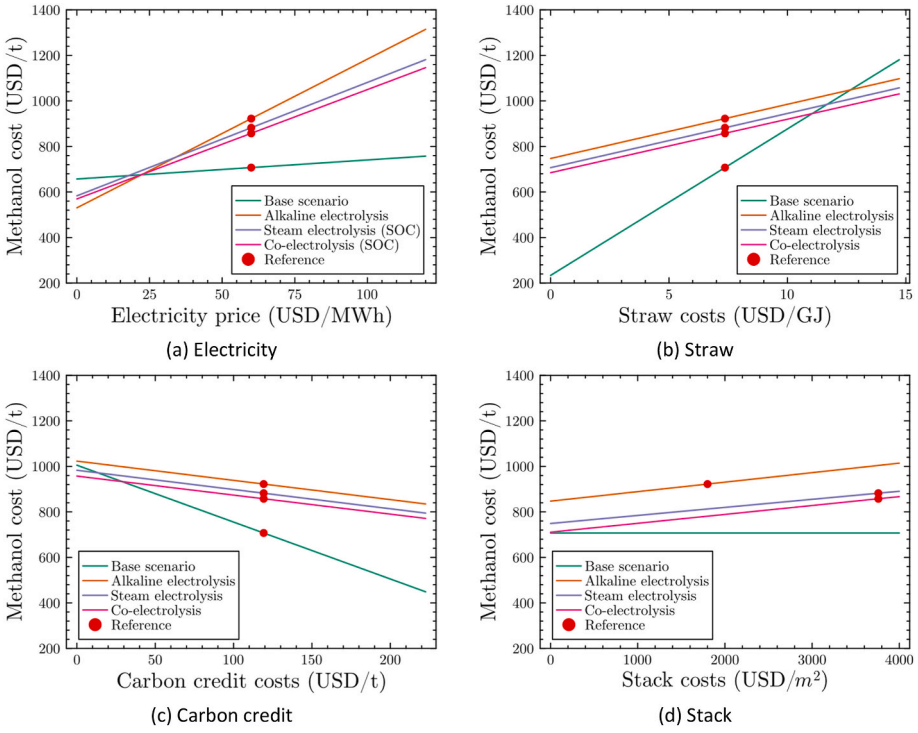

Fig. 12. Influence of electricity, straw, carbon credits and stack costs on methanol costs.

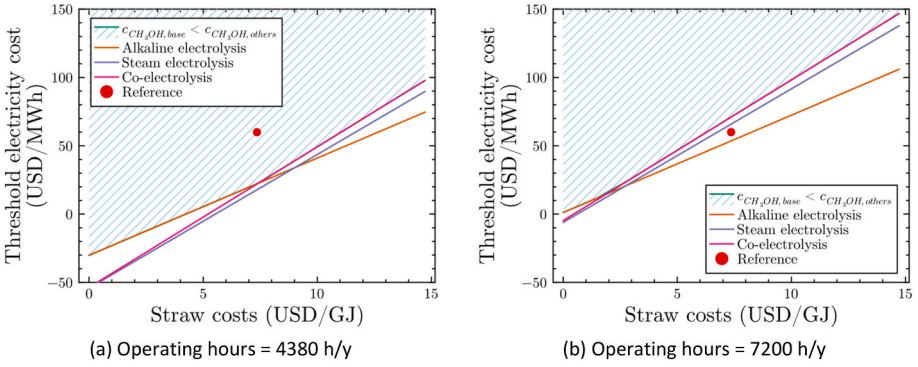

Fig. 13. Maximum electricity costs for which e-bio-methanol costs equals bio-methanol cost.

consumption of pyrolysis gas to supply heat in the base scenario, which lowers the methanol output. Furthermore, other studies have also focused on comparing different alternatives for renewable methanol production in the past. For example, Zhang et al. [14] have estimated energies efficiencies of 49 %, 64 % and 61 % respectively for a bio-methanol plant, steam electrolysis and co-electrolysis combined with gasification. In comparison, our study indicates that co-electrolysis leads to the highest energy efficiency 67.5 % (Definition II), because

Table 9
Comparison of results from this study with literature data.

Reference	Scenario		Main consumption/products			Efficiency		Benchmark
		CAPEX	Biomass	Electricity	Char	Energy	C	cost
		USD/kW$_{CH3OH}$	GJ/t$_{CH3OH}$	MWh/t$_{CH3OH}$	t/t$_{CH3OH}$	%	%	USD/t
This study	Base	3098	64.4	0.84	1.12	55	65	431
	AWE	1862	23.8	6.53	0.41	55	97	660
	SE-SOC	1945	23.8	4.98	0.41	66	97	576
	CE-SOC	1860	23.5	4.80	0.41	67	98	555
[14]	Base	2188	40.1	−0.40	–	53	52[a]	416
	SE-SOC	2214	37.6	–	–	53	55[a]	518
	SE-SOC	2371	20.7	2.84	–	65	100[a]	581
[16]	SE-SOC	941	19.3	2.79	0.03	68	74	404
	CE-SOC	947	15.4	3.56	0.02	71	92	424
[55]	SE-SOC	3083[a]	14.6	3.51	–	68	98	654
	AWE	1809[a]	14.6	5.14	–	57	98	613
[53]	Base	3497	29.8	–	–	67	47	451
	PEM	1769	15.1	5.15	–	62	92	613
[57]	SE-SOC	2174	14.2	4.05	–	69	91	585
	CE-SOC	2001	14.1	4.12	–	69	92	569
	CE-SOC	2327	14.0	4.34	–	67	92	617
	PEM	2333	14.0	5.16	–	62	90	667
[58]	PEM	2077	14.3	5.16	–	60	90	641
	PEM	2413	19.1	3.69	–	61	68	625
	PEM	2483	20.1	3.76	–	59	64	644
[59]	Base	2662	33.2	0.37	0.03	59	37[a]	435
	AWE	2645	25.4	2.87	0.03	56	49[a]	640

[a] Estimated values.

co-electrolysis reduces the heating demand for steam and hot gases. As previously mentioned, pyrolysis does not supply as much heat as gasification, which leads to a heat deficit at high temperatures. A similar result has been reported by Wang et al. [60] for methanol production from CO_2. In contrast, few studies have determined the sources of exergy destruction in bio-e-methanol production, as presented in the previous sections. For instance, Zhang et al. [14] reported an increase in higher methanol costs with an improvement in exergy efficiency for bio-e-methanol plant using biomass gasification, a different pattern than the one observed here for pyrolysis.

The contribution of capital investment to the methanol costs are estimated in this work to range between 203 and 212 USD/t, which are in the lower bound of values estimated by IRENA [10] for bio-methanol from biomass (206–213 USD/t). The large contribution of compressors and heat exchangers presented in Table 8 was also observed by Pérez-Fortes [61] for methanol synthesis using captured CO_2. Furthermore, electrolysis, pyrolysis, compressors, and heat exchangers were also reported as the main equipment costs for a gasification-based bio-e-methanol proposed by Giacomo et al. [16]. The effects of production scale and operating hours shown in Fig. 11 can also be compared with previous investigations. For instance, Zhang et al. [14] have shown a smaller influence of economy of scale for bio-e-methanol plants compared with bio-methanol plants, differently from Fig. 11 (a). However, Zhang et al. [14] have compared the scenarios using the biomass input as basis, and not methanol output. As can be seen from Fig. 11 (a), the scenarios produce different quantities of methanol for the same biomass input, and therefore they have different economy of scale effects when compared on that basis. Furthermore, Poluzzi et al. [54] have also reported similar curve trends as Fig. 11 (b) when varying the electrolyzer capacity factor.

5. Conclusions

This study presents a detailed evaluation of the technical and economic prospects of using pyrolysis combined with different electrolysis technologies to convert biomass into green methanol and biochar. The results indicate that pyrolysis-based systems can have negative direct emissions in methanol production, from −0.62 to −1.02 t_{CO2}/t_{CH3OH}, by co-producing char. This leads to a design that achieves higher carbon utilization for bio-methanol production (65 %), compared with previous studies (e.g., <53 %), and higher energy efficiency (up to 76.5 %) than most bio-e-methanol plants reported in literature (e.g., <71 %), if char is treated as an energy product. In addition, given the revenues from carbon credits associated with its use on soil, char can also reduce methanol costs from 109 to 298 USD/t, which represents roughly 63 % of the biomass consumption costs.

On the other hand, by avoiding char gasification, the methanol plants based on pyrolysis are expected to consume more biomass and electricity, respectively up to 64.4 GJ/t and 4.98 MWh/t. This consequence arises from the fact that char is estimated to contain 45 % of carbon and 48 % of energy available in straw, which could be used for producing methanol, heat, and power. In fact, pinch analysis highlights that, although methanol synthesis can provide heat for distillation and steam generation, there is a lack of heat supply at higher temperature levels (>260 °C) which needs to externally supply from utilities (e.g., syngas burner or electric heater). These possible technical drawbacks can be minimized by using solid oxide electrolysis, which, besides boosting methanol production in 270 % by supplying hydrogen for pyrolysis gas conversion, can also reduce power consumption in 26 % compared to alkaline water electrolysis.

The advantages of integrating solid oxide electrolysis in the proposed designs are further detailed in the exergy analysis. For instance, the scenario using co-electrolysis of water and CO_2 achieves the highest exergy efficiency (78.2 % or 70.1 %, respectively for definitions I and II) due to the lower irreversibilities in high temperature electrolysis and synergies with methanol synthesis and heat integration. These positive interactions between electrolysis in fuel synthesis also translate into reduced heat exchanger sizes and higher conversion ratios of syngas to methanol. Thus, the co-electrolysis scenario has similar fixed capital investment than steam electrolysis (−3%), despite requiring a SOC stack investment 12 % higher.

The economic analysis results indicate a competitive advantage of producing methanol solely from biomass (706 USD/t), mainly due to the lower capital investment and higher capacity factor compared with bio-e-methanol plants (from 856 to 922 USD/t). The solutions adopting electrolysis technology have similar methanol costs (from 856 to 922 USD/t) given the uncertainties in equipment cost estimates (approx. from 109 to 195 USD/t), among which co-electrolysis attains the lowest

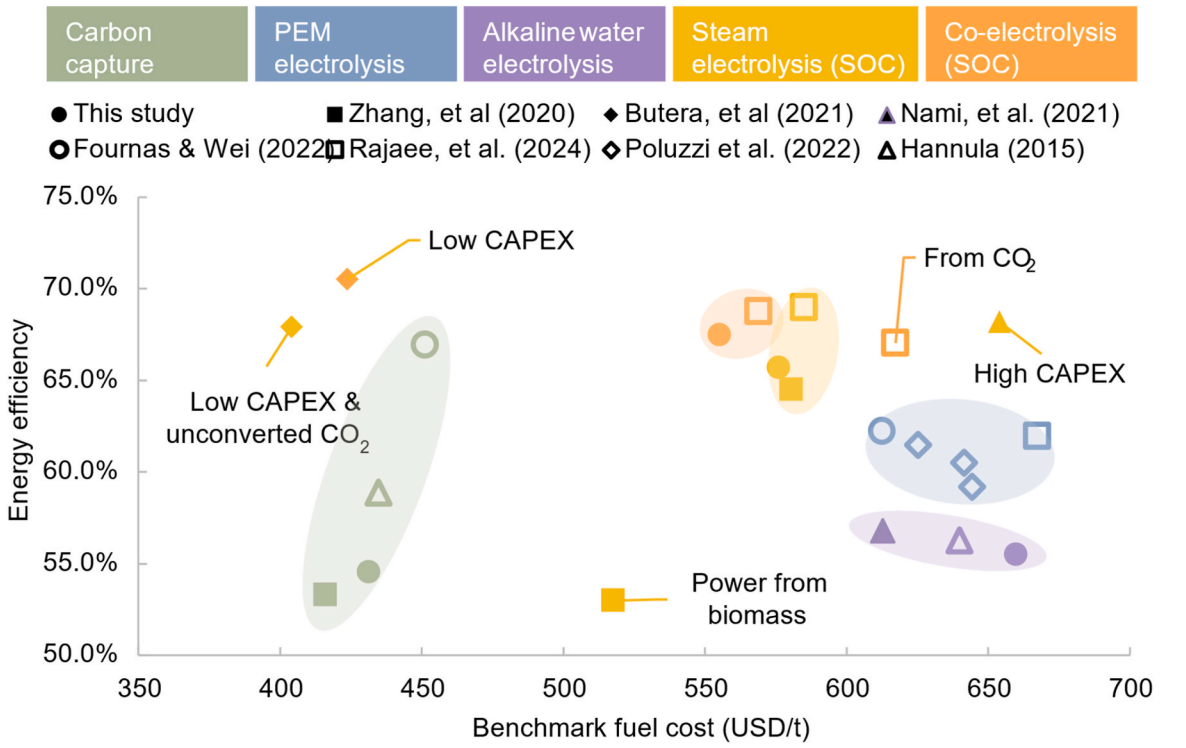

(a) Energy efficiency (definition II) vs. benchmark cost

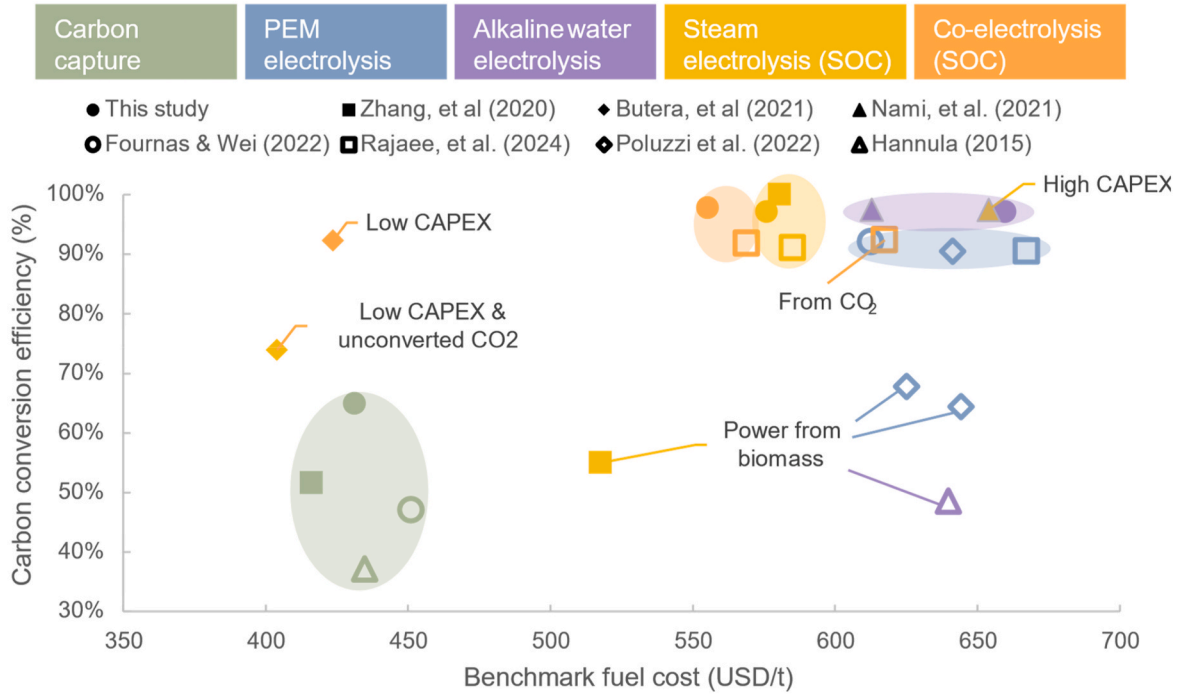

(b) Carbon conversion efficiency vs. benchmark cost

Fig. 14. Comparison of techno-economic results for bio-methanol and bio-e-methanol in literature [14,16,53,55,57–59]. (Symbols and colors represent references and technology type, respectively). (For interpretation of the references to color in this figure legend, the reader is referred to the Web version of this article.)

value. Data from previous studies were compiled and compared under the same economic assumptions by a proposed benchmark cost metric. The study shows clear clusters of solutions related to technology adopted. In general, bio-e-methanol are more expensive (min. +100 USD/t), have higher carbon conversion (>90 %) and solutions based on SOC technology are more energy efficient (>65 %) and less expensive than PEM and AWE (up to 100 USD/t lower). The pyrolysis-based system proposed in this study shows high carbon conversion efficiency and lower costs compared to most of previous literature.

CRediT authorship contribution statement

Rafael Nogueira Nakashima: Writing – review & editing, Writing – original draft, Validation, Software, Methodology, Formal analysis, Conceptualization. **Hossein Nami:** Writing – review & editing, Methodology. **Arash Nemati:** Writing – review & editing, Conceptualization. **Giacomo Butera:** Writing – review & editing, Software, Methodology. **Silvio de Oliveira Junior:** Writing – review & editing, Methodology. **Peter Vang Hendriksen:** Writing – review & editing, Supervision, Project administration, Conceptualization. **Henrik Lund Frandsen:** Writing – review & editing, Writing – original draft, Supervision.

Declaration of competing interest

The authors declare the following financial interests/personal relationships which may be considered as potential competing interests: Rafael Nogueira Nakashima reports financial support was provided by Danish Energy Agency. Silvio de Oliveira Junior reports financial support was provided by National Council for Scientific and Technological Development. Giacomo Butera reports a relationship with Stiesdal that includes: employment. If there are other authors, they declare that they have no known competing financial interests or personal relationships that could have appeared to influence the work reported in this paper.

Acknowledgments

The authors would like to acknowledge Lasse Røngaard Clausen for his contributions in the development of the pyrolysis model. The authors wish to thank the Energy Technology Development and Demonstration Program (EUDP) at the Danish Energy Agency for financial support via the "SkyClean 2 MW Process Development and Industrial Demonstration" project (project no. 64021-1114). The sixth author acknowledges CNPq (Brazilian National Council for Scientific and Technological Development) for the grant 306484/2020-0.

Appendix B. Supplementary data

Supplementary data to this article can be found online at https://doi.org/10.1016/j.renene.2025.122388.

Appendix A. Model assumptions and parameters

Table A 1
Pyrolysis unit assumptions and parameters

Parameter	Value	Unit
Straw		
Composition	47.29 % C, 5.64 % H, 41.25 % O, 0.67 % N and 5.15 % ash	wt.% (dry basis)
Moisture	10 %	wt. %
Higher heating value	18.3	MJ/kg (dry basis)
Specific heat capacity	1.35	kJ/kg K
Char		
Composition	71.8 % C, 2.85 % H, 5.39 % O, 2.30 % N and 17.66 % ash	wt.% (dry basis)
Moisture	0	wt.%
Higher heating value	28.26	MJ/kg (dry basis)
Specific heat capacity	1	kJ/kg
Pyrolysis gas		
Composition	8.19 % H_2, 27.87 % H_2O, 7.28 % CO, 31.92 % CO_2, 21.09 % CH_4, 0.84 % C_2H_4, 1.82 % C_2H_6, 0.59 % C_3H_6, 0.40 % C_3H_8	mol % (dry basis)
Others		
Inert consumption	0.05	kg/kg_{straw}
Heat loss	0.02	$kJ/kJ_{straw\text{-}LHV}$
Pressure drop (reactor)	3	kPa
Fan isentropic efficiency	70 %	
Fan mechanical efficiency	95 %	

Table A 2
Reforming unit assumptions and parameters

Parameter	Value	Unit
Reformer		
Inlet pressure	1.05	bar
Inlet temperature	800	°C
O/C molar ratio	1.89	
Others		
Sulfur removal efficiency	100 %	

Table A 3
Amine absorption unit assumptions and parameters.

Parameter/Assumption	Value	Unit
Water gas shift		
Pressure	15	bar
Inlet temperature	350	°C
Inlet S/C ratio	1.19	
CO_2 separation		
Packing vendor/material (Absorber & Stripper)	Generic/Plastic	
Packing dimensions (Absorber & Stripper)	16	mm
Stripper - condenser type	Partial-Vapor	
Stripper – condenser temperature	45	°C
Stripper – reboiler type	Kettle	
Stripper – feeding stage	2	

Table A 4
Electrolysis unit assumptions and parameters

Parameter/Assumption	Value	Unit
Stack inlet temperature	750	°C
Stack inlet pressure	1.05	bar
Minimal inlet molar fraction of H_2	0.1	
Operating cell voltage – Steam electrolysis	1.2852	V (thermoneutral)
Operating cell voltage – Co-electrolysis	1.3125	V (thermoneutral)
Feedstock utilization efficiency	0.7	
Pressure loss – SOEC stack	0.03	bar
Excess oxygen flow	200	% stoichiometric O_2
Rectifier AC/DC efficiency [62]	95	%
Ejector efficiency [63]	10	%

Table A 5
Electrochemistry model parameters [8,64].

Parameter	Value	Unit
Cathode/anode/electrolyte thickness	350/40/10	μm
Cathode/anode porosity	0.31/0.40	
Cathode/anode tortuosity	2.52	
Cathode/anode mean pore diameter	$6.41 \times 10^{-7}/3.06 \times 10^{-7}$	m

Table A 6
Methanol synthesis unit assumptions and parameters

Parameter/Assumption	Value	Unit
Methanol reactor temperature	265	°C
Methanol reactor pressure	90	bar
Recycle ratio in methanol synthesis	0.99	–
Reflux ratio		
Topping	0.9	
Distillation	0.8	
Tray spacing	0.61	m
Reboiler type (Topping & distillation)	Kettle	

Table A 7
Utilities assumptions and parameters.

Parameter	Value	Unit
Burner		
Air preheating temperature	125	°C
Percentage of stoichiometric air [65]	115 % (for gases) 125 % (for solids)	
Exhaust gases temperature	160	°C
Burner pressure drop	0.04	bar
Burner heat losses	3 % combustion heat [65]	
Others		

(*continued on next page*)

Table A 7 (*continued*)

Parameter	Value	Unit
Fan/Pump isentropic efficiency	70 %	
Fan/Pump mechanical efficiency	95 %	
Specific power consumption – cooling tower	14.3 [41]	W/kW_{heat}
Electric heating efficiency	100 %	
Specific power consumption – air separation unit	160 [14]	kWh/t_{O2}

References

[1] H. Wenzel, Biomass Availability and Sector Competition, University of Southern Denmark, Denmark, 2022.
[2] Mærsk Mc-Kinney Møller Center, Position Paper Fuel Option Scenarios, 2021. Denmark.
[3] S.M. Franz, S. Shapiro-Bengtsen, N.J.B. Campion, M. Backer, M. Münster, MarE-Fuel: ROADMAP for Sustainable Maritime Fuels, Technical University of Denmark, 2021.
[4] R. Nogueira Nakashima, D. Flórez-Orrego, H.I. Velásquez, S. De Oliveira Junior, Sugarcane bagasse and vinasse conversion to electricity and biofuels: an exergoeconomic and environmental assessment, IJEX 33 (2020) 44, https://doi.org/10.1504/IJEX.2020.109623.
[5] L.R. Clausen, Maximizing biofuel production in a thermochemical biorefinery by adding electrolytic hydrogen and by integrating torrefaction with entrained flow gasification, Energy 85 (2015) 94–104, https://doi.org/10.1016/j.energy.2015.03.089.
[6] Domingos MEG. Ribeiro, D. Flórez-Orrego, M. Teles dos Santos, S. de Oliveira, F. Maréchal, Techno-economic and environmental analysis of methanol and dimethyl ether production from syngas in a kraft pulp process, Comput. Chem. Eng. 163 (2022) 107810, https://doi.org/10.1016/j.compchemeng.2022.107810.
[7] IEA, The Future of Hydrogen, IEA, Paris, 2019.
[8] H. Nami, O.B. Rizvandi, C. Chatzichristodoulou, P.V. Hendriksen, H.L. Frandsen, Techno-economic analysis of current and emerging electrolysis technologies for green hydrogen production, Energy Convers. Manag. 269 (2022) 116162, https://doi.org/10.1016/j.enconman.2022.116162.
[9] IRENA, Green Hydrogen Cost Reduction: Scaling up Electrolysers to Meet the 1.5^0 C Climate Goal, Irena, Abu Dhabi, 2020.
[10] IRENA, Methanol Institute, Innovation Outlook : Renewable Methanol, International Renewable Energy Agency, Abu Dhabi, 2021.
[11] L. Tock, M. Gassner, F. Maréchal, Thermochemical production of liquid fuels from biomass: thermo-economic modeling, process design and process integration analysis, Biomass Bioenergy 34 (2010) 1838–1854, https://doi.org/10.1016/j.biombioe.2010.07.018.
[12] J. Lebaek, J. Boegild Hansen, M. Mogensen, GreenSynFuels. Economical and technological statement regarding integration and storage of renewable energy in the energy sector by production of green synthetic fuels for utilization in fuel cells, Final project report, 2011, p. 84.
[13] S. Ali, K. Sørensen, M.P. Nielsen, Modeling a novel combined solid oxide electrolysis cell (SOEC) - biomass gasification renewable methanol production system, Renew. Energy 154 (2020) 1025–1034, https://doi.org/10.1016/j.renene.2019.12.108.
[14] H. Zhang, L. Wang, M. Pérez-Fortes, J. Van herle, F. Maréchal, U. Desideri, Techno-economic optimization of biomass-to-methanol with solid-oxide electrolyzer, Appl. Energy 258 (2020) 114071, https://doi.org/10.1016/j.apenergy.2019.114071.
[15] G. Butera, S. Højgaard Jensen, R. Østergaard Gadsbøll, J. Ahrenfeldt, L. Røngaard Clausen, Flexible biomass conversion to methanol integrating solid oxide cells and TwoStage gasifier, Fuel 271 (2020) 117654, https://doi.org/10.1016/j.fuel.2020.117654.
[16] G. Butera, S.H. Jensen, J. Ahrenfeldt, L.R. Clausen, Techno-economic analysis of methanol production units coupling solid oxide cells and thermochemical biomass conversion via the TwoStage gasifier, Fuel Process. Technol. 215 (2021) 106718, https://doi.org/10.1016/j.fuproc.2020.106718.
[17] Ministry of Food, Agriculture and Fisheries of Denmark. Emissions from the agricultural sector will be reduced by 55 to 65 percent, Denmark: Ministry of Food, Agriculture and Fisheries of Denmark (2021).
[18] Puro Earth, Puro Standard: Biochar Methodology, Finland, 2023.
[19] J. Nepal, W. Ahmad, F. Munsif, A. Khan, Z. Zou, Advances and prospects of biochar in improving soil fertility, biochemical quality, and environmental applications, Front. Environ. Sci. 11 (2023) 1114752, https://doi.org/10.3389/fenvs.2023.1114752.
[20] R.Ø. Gadsbøll, L.R. Clausen, T.P. Thomsen, J. Ahrenfeldt, U.B. Henriksen, Flexible TwoStage biomass gasifier designs for polygeneration operation, Energy 166 (2019) 939–950, https://doi.org/10.1016/j.energy.2018.10.144.
[21] S.A. Klein, Engineering Equation Solver (EES), United States of America: F-Chart Software, 2022.
[22] F. Marechal, F. Palazzi, J. Godat, D. Favrat, Thermo-economic modelling and optimisation of fuel cell systems, Fuel Cell. 5 (2005) 5–24, https://doi.org/10.1002/fuce.200400055.
[23] ASPENTECH. Aspen Plus, Bedford, United States, Aspen technology Inc., 2015.
[24] A.A. Kiss, J.J. Pragt, H.J. Vos, G. Bargeman, M.T. de Groot, Novel efficient process for methanol synthesis by CO 2 hydrogenation, Chem. Eng. J. 284 (2016) 260–269, https://doi.org/10.1016/j.cej.2015.08.101.
[25] Aspen Technology, Inc. Rate-Based Model of the CO2 Capture Process by MEA Using Aspen Plus, Aspen Technolgy, Inc., Bedford, United States, 2014.
[26] Aspen Technology, Inc. Rate-Based Model of the CO2 Capture Process by MDEA Using Aspen Plus, Aspen Technolgy, Inc., Bedford, United States, 2014.
[27] L. Jin, R. Nogueira Nakashima, G. Comodi, H.L. Frandsen, Alkaline electrolysis for green hydrogen production: techno-economic analysis of temperature influence and control. Proceedings of the 36th International Conference on Efficiency, Cost, Optimization, Simulation and Environmental Impact of Energy Systems, Las Palmas de Gran Canaria, Spain, 2023.
[28] O. Ulleberg, Modeling of advanced alkaline electrolyzers: a system simulation approach, Int. J. Hydrogen Energy 28 (2003) 21–33, https://doi.org/10.1016/S0360-3199(02)00033-2.
[29] A. Nemati, O.B. Rizvandi, F. Mondi, H.L. Frandsen, Detailed 3D multiphysics modeling of an ammonia-fueled solid oxide fuel cell: anode off-gas recirculation and Ni nitriding degradation, Energy Convers. Manag. 308 (2024) 118396, https://doi.org/10.1016/j.enconman.2024.118396.
[30] R. Nogueira Nakashima, S. De Oliveira, Thermodynamic evaluation of solid oxide fuel cells converting biogas into hydrogen and electricity, Int. J. Therm. 24 (2021) 204–214, https://doi.org/10.5541/ijot.877847.
[31] R. Nogueira Nakashima, S. Oliveira Junior, Multi-objective optimization of biogas systems producing hydrogen and electricity with solid oxide fuel cells, Int. J. Hydrogen Energy S036031992103442X (2021), https://doi.org/10.1016/j.ijhydene.2021.08.195.
[32] C. Bao, Z. Jiang, X. Zhang, Modeling mass transfer in solid oxide fuel cell anode: I. Comparison between Fickian, Stefan-Maxwell and dusty-gas models, J. Power Sources 310 (2016) 32–40, https://doi.org/10.1016/j.jpowsour.2016.01.099.
[33] B.A. Haberman, J.B. Young, Three-dimensional simulation of chemically reacting gas flows in the porous support structure of an integrated-planar solid oxide fuel cell, Int. J. Heat Mass Tran. 47 (2004) 3617–3629, https://doi.org/10.1016/j.ijheatmasstransfer.2004.04.010.
[34] C. Rackauckas, Q. Nie, Differentialequations.jl–a performant and feature-rich ecosystem for solving differential equations in julia, J. Open Res. Software 5 (2017), https://doi.org/10.5334/jors.151.
[35] T. Blumberg, T. Morosuk, G. Tsatsaronis, Exergy-based evaluation of methanol production from natural gas with CO2 utilization, Energy 141 (2017) 2528–2539, https://doi.org/10.1016/j.energy.2017.06.140.
[36] K.M.V. Bussche, G.F. Froment, A steady-state kinetic model for methanol synthesis and the water gas shift reaction on a commercial Cu/ZnO/Al2O3Catalyst, J. Catal. 161 (1996) 1–10, https://doi.org/10.1006/jcat.1996.0156.
[37] Aspen Technology, Inc. Aspen Plus Methanol Synthesis Mode. Bedford, United States: Aspen Technolgy, Inc.; 2018.
[38] F. Marechal, B. Kalitventzeff, Targeting the minimum cost of energy requirements: a new graphical technique for evaluating the integration of utility systems, Comput. Chem. Eng. 20 (1996) S225–S230, https://doi.org/10.1016/0098-1354(96)00048-8.
[39] R.N. Nakashima, Modelling, Simulation and Optimization of Biogas Conversion Routes Integrated with Fuel Cell Technology, Universidade de São Paulo, 2022, https://doi.org/10.11606/T.3.2022.tde-26082022-081436. PhD thesis.
[40] P. Voll, C. Klaffke, M. Hennen, A. Bardow, Automated superstructure-based synthesis and optimization of distributed energy supply systems, Energy 50 (2013) 374–388, https://doi.org/10.1016/j.energy.2012.10.045.
[41] R. Turton, R.C. Bailie, W.B. Whiting, J.A. Shaeiwitz, Analysis, Synthesis, and Design of Chemical Processes, 3th ed., Prentice Hall, Upper Saddle River, NJ, 2009.
[42] S. de Oliveira Junior, Exergy: Production, Cost and Renewability, Springer London, London, 2013, https://doi.org/10.1007/978-1-4471-4165-5.
[43] T.-V. Nguyen, L.R. Clausen, Techno-economic analysis of polygeneration systems based on catalytic hydropyrolysis for the production of bio-oil and fuels, Energy Convers. Manag. 184 (2019) 539–558, https://doi.org/10.1016/j.enconman.2019.01.070.
[44] Federal Research System, Statement on longer-run goals and monetary policy strategy. Review of monetary policy strategy, tools, and communications 2020. https://www.federalreserve.gov/monetarypolicy/review-of-monetary-policy-strategy-tools-and-communications-statement-on-longer-run-goals-monetary-policy-strategy.htm, 2020.
[45] R.H. Perry, D.W. Green, J.O. Maloney (Eds.), Perry's Chemical Engineers' Handbook, seventh ed., McGraw-Hill, New York, 1997.
[46] W.D. Seider, D.R. Lewin, J.D. Seader, S. Widagdo, R. Gani, K.M. Ng, Product and Process Design Principles: Synthesis, Analysis and Evaluation, fourth ed., Wiley, New York, 2017.

[47] C. Maxwell, Cost Indices, Towering Skills, 2023. https://toweringskills.com/financial-analysis/cost-indices/.
[48] Chemical Engineering magazine, The Chemical Engineering Plant Cost Index, 2021.
[49] C. Hodgson, D. Sheppard, EU Carbon Price Tops €100 a Tonne for First Time, Financial Times, 2023.
[50] IRENA, Renewable Power Generation Costs in 2022, International Renewable Energy Agency, Abu Dhabi, 2023.
[51] Danmarks Nationalbank, Exchange rates. Exchange rates. https://www.nationalbanken.dk/en/news-and-knowledge/data-and-statistics/exchange-rates, 2023.
[52] European Central Bank, Euro foreign exchange reference rates. https://www.ecb.europa.eu/stats/policy_and_exchange_rates/euro_reference_exchange_rates/html/index.en.html, 2023.
[53] N. de Fournas, M. Wei, Techno-economic assessment of renewable methanol from biomass gasification and PEM electrolysis for decarbonization of the maritime sector in California, Energy Convers. Manag. 257 (2022) 115440, https://doi.org/10.1016/j.enconman.2022.115440.
[54] A. Poluzzi, G. Guandalini, S. Guffanti, C. Elsido, S. Moioli, P. Huttenhuis, et al., Flexible Power & Biomass-to-Methanol plants: design optimization and economic viability of the electrolysis integration, Fuel 310 (2022) 122113, https://doi.org/10.1016/j.fuel.2021.122113.
[55] H. Nami, G. Butera, N.J.B. Campion, H.L. Frandsen, P.V. Hendriksen, MarE-fuel: Energy Efficiencies in Synthesising Green Fuels and Their Expected Cost, Technical University of Denmark, Denmark, 2021.
[56] H. Liu, L.R. Clausen, L. Wang, M. Chen, Pathway toward cost-effective green hydrogen production by solid oxide electrolyzer, Energy Environ. Sci. 16 (2023) 2090–2111, https://doi.org/10.1039/D3EE00232B.
[57] F. Rajaee, G. Guandalini, M.C. Romano, J. Ritvanen, Techno-economic evaluation of biomass-to-methanol production via circulating fluidized bed gasifier and solid oxide electrolysis cells: a comparative study, Energy Convers. Manag. 301 (2024) 118009, https://doi.org/10.1016/j.enconman.2023.118009.
[58] A. Poluzzi, G. Guandalini, S. Guffanti, M. Martinelli, S. Moioli, P. Huttenhuis, et al., Flexible power and biomass-to-methanol plants with different gasification technologies, Front. Energy Res. 9 (2022) 795673, https://doi.org/10.3389/fenrg.2021.795673.
[59] I. Hannula, Co-production of synthetic fuels and district heat from biomass residues, carbon dioxide and electricity: performance and cost analysis, Biomass Bioenergy 74 (2015) 26–46, https://doi.org/10.1016/j.biombioe.2015.01.006.
[60] L. Wang, M. Chen, R. Küngas, T.-E. Lin, S. Diethelm, F. Maréchal, et al., Power-to-fuels via solid-oxide electrolyzer: operating window and techno-economics, Renew. Sustain. Energy Rev. 110 (2019) 174–187, https://doi.org/10.1016/j.rser.2019.04.071.
[61] M. Pérez-Fortes, J.C. Schöneberger, A. Boulamanti, E. Tzimas, Methanol synthesis using captured CO2 as raw material: techno-economic and environmental assessment, Appl. Energy 161 (2016) 718–732, https://doi.org/10.1016/j.apenergy.2015.07.067.
[62] Ro Peters, W. Tiedemann, I. Hoven, R. Deja, N. Kruse, Q. Fang, et al., Experimental results of a 10/40 kW-class reversible solid oxide cell demonstration system at forschungszentrum jülich, J. Electrochem. Soc. 170 (2023) 044509, https://doi.org/10.1149/1945-7111/accbf0.
[63] Y. Huang, P. Jiang, Y. Zhu, Quasi-two-dimensional ejector model for anode gas recirculation fuel cell systems, Energy Convers. Manag. 262 (2022) 115674, https://doi.org/10.1016/j.enconman.2022.115674.
[64] L. Wang, M. Rao, S. Diethelm, T.-E. Lin, H. Zhang, A. Hagen, et al., Power-to-methane via co-electrolysis of H2O and CO2: the effects of pressurized operation and internal methanation, Appl. Energy 250 (2019) 1432–1445, https://doi.org/10.1016/j.apenergy.2019.05.098.
[65] R. Smith, Chemical Process Design and Integration, Wiley, Chichester, West Sussex, England ; Hoboken, NJ, 2005.